REFERENCES

3.1. McRuer, D.; I. Ashkemas; and D. Graham. *Aircraft Dynamics and Automatic Control.* Princeton, NJ: Princeton University Press, 1973.

3.2. Bryan, G. H.; and W. E. Williams. "The Longitudinal Stability of Aerial Gliders." *Proceedings of the Royal Society of London, Series A* 73 (1904), pp. 110–116.

3.3. Bryan, G. H. *Stability in Aviation.* London: Macmillan, 1911.

3.4. *USAF Stability and Control DATCOM*, Flight Control Division, Air Force Flight Dynamics Laboratory, Wright-Patterson Air Force Base, Fairborn, OH.

3.5. Smetana, F. O.; D. C. Summey; and W. D. Johnson. *Riding and Handling Qualities of Light Aircraft—A Review and Analysis.* NASA CR-1955, March 1972.

3.6. MacDonald, R. A.; M. Garelick; and J. O'Grady. "Linearized Mathematical Models for DeHavilland Canada 'Buffalo and Twin Otter' STOL Transports." U.S. Department of Transportation, Transportation Systems Center Report No. DOT-TSC-FAA-71-8, June 1971.

CHAPTER 4

Longitudinal Motion (Stick Fixed)

"The equilibrium and stability of a bird in flight, or an aerodome or flying machine, has in the past been the subject of considerable speculation, and no adequate explanation of the principles involved has hitherto been given."

Frederick W. Lanchester, *Aerodonetics* [4.1], published in 1908, in which he develops an elementary theory of longitudinal dynamic stability.

4.1 HISTORICAL PERSPECTIVE

The theoretical basis for the analysis of flight vehicle motion developed almost concurrently with the successful demonstration of a powered flight of a human-carrying airplane. As early as 1897, Frederick Lanchester was studying the motion of gliders. He conducted experiments with hand-launched gliders and found that his gliders would fly along a straight path if they were launched at what he called the glider's natural speed. Launching the glider at a higher or lower speed would result in an oscillatory motion. He also noticed that, if launched at its "natural speed" and then disturbed from its flight path, the glider would start oscillating along its flight trajectory. What Lanchester had discovered was that all flight vehicles possess certain natural frequencies or motions when disturbed from their equilibrium flight.

Lanchester called the oscillatory motion the phugoid motion. He wanted to use the Greek word meaning "to fly" to describe his newly discovered motion; actually, phugoid means "to flee." Today, we still use the term phugoid to describe the long-period slowly damped oscillation associated with the longitudinal motion of an airplane.

The mathematical treatment of flight vehicle motions was first developed by G. H. Bryan. He was aware of Lanchester's experimental observations and set out to develop the mathematical equations for dynamic stability analysis. His stability work was published in 1911. Bryan made significant contributions to the analysis of vehicle flight motion. He laid the mathematical foundation for airplane dynamic stability analysis, developed the concept of the aerodynamic stability derivative, and recognized that the equations of motion could be separated into a symmetric longitudinal motion and an unsymmetric lateral motion. Although the mathematical treatment of airplane dynamic stability was formulated shortly after the first

successful human-controlled flight, the theory was not used by the inventors because of its mathematical complexity and the lack of information on the stability derivatives.

Experimental studies were initiated by L. Bairstow and B. M. Jones of the National Physical Laboratory (NPL) in England and Jerome Hunsaker of the Massachusetts Institute of Technology (MIT) to determine estimates of the aerodynamic stability derivatives used in Bryan's theory. In addition to determining stability derivatives from wind-tunnel tests of scale models, Bairstow and Jones nondimensionalized the equations of motion and showed that, with certain assumptions, there were two independent solutions; that is, one longitudinal and one lateral. During the same period, Hunsaker and his group at MIT conducted wind-tunnel studies of scale models of several flying airplanes. The results from these early studies were extremely valuable in establishing relationships between aerodynamics, geometric and mass characteristics of the airplanes, and its dynamic stability.*

Although these early investigators could predict the stability of the longitudinal and lateral motions, they were unsure how to interpret their findings. They were preplexed because when their analysis predicted an airplane would be unstable the airplane was flown successfully. They wondered how the stability analysis could be used to assess whether an airplane was of good or bad design. The missing factor in analyzing airplane stability in these early studies was the consideration of the pilot as an essential part of the airplane system.

In the late 1930s the National Advisory Committee of Aeronautics (NACA) conducted an extensive flight test program. Many airplanes were tested with the goal of quantitatively relating the measured dynamic characteristics of the airplane with the pilot's opinion of its handling characteristics. These experiments laid the foundation for modern flying qualities research. In 1943, R. Gilruth reported the results of the NACA research program in the form of flying qualities' specifications. For the first time, the designer had a list of specifications that could be used in designing the airplane. If the design complied with the specifications, one could be reasonably sure that the airplane would have good flying qualities [4.1–4.4].

In this chapter we shall examine the longitudinal motion of an airplane disturbed from its equilibrium state. Several different analytical techniques will be presented for solving the longitudinal differential equations. Our objectives are for the student to understand the various analytical techniques employed in airplane motion analysis and to appreciate the importance of aerodynamic or configuration changes on the airplane's dynamic stability characteristics. Later we shall discuss what constitutes good flying qualities in terms of the dynamic characteristics presented here. Before attempting to solve the longitudinal equations of motion, we will examine the solution of a simplified aircraft motion. By studying the simpler motions with a single degree of freedom, we shall gain some insight into the more complicated longitudinal motions we shall study later in this chapter.

* The first technical report by the National Advisory Committee of Aeronautics, NACA (forerunner of the National Aeronautics and Space Administration, NASA), summarizes the MIT research in dynamic stability.

4.2 SECOND-ORDER DIFFERENTIAL EQUATIONS

Many physical systems can be modeled by second-order differential equations. For example, control servomotors, special cases of aircraft dynamics, and many electrical and mechanical systems are governed by second-order differential equations. Because the second-order differential equation plays such an important role in aircraft dynamics we shall examine its characteristics before proceeding with our discussion of aircraft motions.

To illustrate the properties of a second-order differential equation, we examine the motion of a mechanical system composed of a mass, a spring, and a damping device. The forces acting on the system are shown in Figure 4.1. The spring provides a linear restoring force that is proportional to the extension of the spring, and the damping device provides a damping force that is proportional to the velocity of the mass. The differential equation for the system can be written as

$$m\frac{d^2x}{dt^2} + c\frac{dx}{dt} + kx = F(t) \tag{4.1}$$

or

$$\frac{d^2x}{dt^2} + \frac{c}{m}\frac{dx}{dt} + \frac{k}{m}x = \frac{1}{m}F(t) \tag{4.2}$$

This is a nonhomogeneous, second-order differential equation with constant coefficients. The coefficients in the equation are determined from the physical characteristics of the mechanical system being modeled, that is, its mass, damping coefficient, and spring constant. The function $F(t)$ is called the forcing function. If the forcing function is 0, the response of the system is referred to as the free response. When the system is driven by a forcing function $F(t)$ the response is referred to as the forced response. The general solution of the nonhomogeneous differential equation is the sum of the homogeneous and particular solutions. The homogeneous solution is the solution of the differential equation when the right-hand side of the equation is 0. This corresponds to the free response of the system. The particular solution is a solution that when substituted into the left-hand side of the

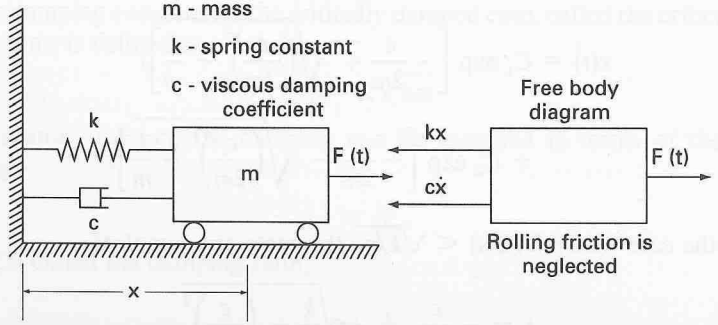

FIGURE 4.1
A spring mass damper system.

differential equation yields the nonhomogeneous or right-hand side of the differential equation. In the following section we will restrict our discussion to the solution of the free response or homogeneous equation.

The solution of the differential equation with constant coefficients is found by letting

$$x = Ae^{\lambda t} \tag{4.3}$$

and substituting into the differential equation yields

$$\lambda^2 Ae^{\lambda t} + \frac{c}{m}\lambda Ae^{\lambda t} + \frac{k}{m}Ae^{\lambda t}e = 0 \tag{4.4}$$

Clearing the equation of $Ae^{\lambda t}$ yields

$$\lambda^2 + \frac{c}{m}\lambda + \frac{k}{m} = 0 \tag{4.5}$$

which is called the characteristic equation. The roots of the characteristic equation are called the characteristic roots or eigenvalues of the system.

The roots of Equation (4.5) are

$$\lambda_{1,2} = -\frac{c}{2m} \pm \sqrt{\left(\frac{c}{2m}\right)^2 - \frac{k}{m}} \tag{4.6}$$

The solution of the differential equation can now be written as

$$x(t) = C_1 e^{\lambda_1 t} + C_2 e^{\lambda_2 t} \tag{4.7}$$

where C_1 and C_2 are arbitrary constants determined from the initial conditions of the problem. The type of motion that occurs if the system is displaced from its equilibrium position and released depends on the value of λ. But λ depends on the physical constants of the problem; namely, m, c, and k. We shall consider three possible cases for λ.

When $(c/2m) > \sqrt{k/m}$, the roots are negative and real, which means that the motion will die out exponentially with time. This type of motion is referred to as an overdamped motion. The equation of motion is given by

$$x(t) = C_1 \exp\left[-\frac{c}{2m} + \sqrt{\left(\frac{c}{2m}\right)^2 - \frac{k}{m}}\right]t + C_2 \exp\left[-\frac{c}{2m} - \sqrt{\left(\frac{c}{2m}\right)^2 - \frac{k}{m}}\right]t \tag{4.8}$$

For the case where $(c/2m) < \sqrt{k/m}$, the roots are complex:

$$\lambda = -\frac{c}{2m} \pm i\sqrt{\frac{k}{m} - \left(\frac{c}{2m}\right)^2} \tag{4.9}$$

The equation of motion is as follows:

$$x(t) = \exp\left(-\frac{c}{2m}t\right)\left[C_1 \exp\left[i\sqrt{\frac{k}{m} - \left(\frac{c}{2m}\right)^2}\,t\right] + C_2 \exp\left[-i\sqrt{\frac{k}{m} - \left(\frac{c}{2m}\right)^2}\,t\right]\right] \tag{4.10}$$

which can be rewritten as

$$x(t) = \exp\left(-\frac{c}{2m}t\right)\left[A\cos\left[\sqrt{\frac{k}{m} - \left(\frac{c}{2m}\right)^2}\,t\right] + B\sin\left[\sqrt{\frac{k}{m} - \left(\frac{c}{2m}\right)^2}\,t\right]\right] \tag{4.11}$$

The solution given by Equation (4.11) is a damped sinusoid having a natural frequency given by

$$\omega = \sqrt{\frac{k}{m} - \left(\frac{c}{2m}\right)^2} \tag{4.12}$$

The last case we consider is when $(c/2m) = \sqrt{k/m}$. This represents the boundary between the overdamped exponential motion and the damped sinusoidal motion. This particular motion is referred to as the critically damped motion. The roots of the characteristic equation are identical; that is,

$$\lambda_{1,2} = -\frac{c}{2m} \tag{4.13}$$

The general solution for repeated roots has the form

$$x(t) = (C_1 + C_2 t)\, e^{\lambda t} \tag{4.14}$$

If λ is a negative constant, then $e^{\lambda t}$ will go to 0 faster than $C_2 t$ goes to infinity as time increases. Figure 4.2 shows the motion for the three cases analyzed here.

The damping constant for the critically damped case, called the critical damping constant, is defined as

$$c_{cr} = 2\sqrt{km} \tag{4.15}$$

For oscillatory motion, the damping can be specified in terms of the critical damping:

$$c = \zeta c_{cr} \tag{4.16}$$

where ζ is called the damping ratio,

$$\zeta = \frac{c}{c_{cr}} \tag{4.17}$$

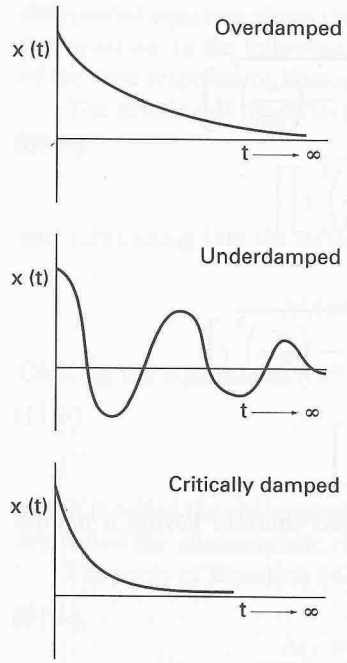

FIGURE 4.2
Typical motions of a dynamic system.

For a system that has no damping, that is, $c = 0$, which implies that $\zeta = 0$, the motion is an undamped oscillation. The natural frequency, called the undamped natural frequency, can be obtained from Equation (4.12) by setting $c = 0$:

$$\omega_n = \sqrt{\frac{k}{m}} \tag{4.18}$$

Since both the damping ratio and undamped natural frequency are specified as functions of the system physical constants, we can rewrite the differential equation in terms of the damping ratio and undamped natural frequency as follows:

$$\frac{d^2x}{dt^2} + 2\zeta\omega_n \frac{dx}{dt} + \omega_n^2 x = f(t) \tag{4.19}$$

Equation (4.19) is the standard form of a second-order differential equation with constant coefficients. Although we developed the standard form of a second-order differential equation from a mechanical mass-spring-damper system, the equation could have been developed using any one of an almost limitless number of physical systems. For example, a torsional spring-mass-damper equation of motion is given by

$$\frac{d^2\theta}{dt^2} + \frac{c}{I}\frac{d\theta}{dt} + \frac{k}{I}\theta = f(t) \tag{4.20}$$

where c, k, and I are the torsional damping coefficient, torsional spring constant, and moment of inertia, respectively.

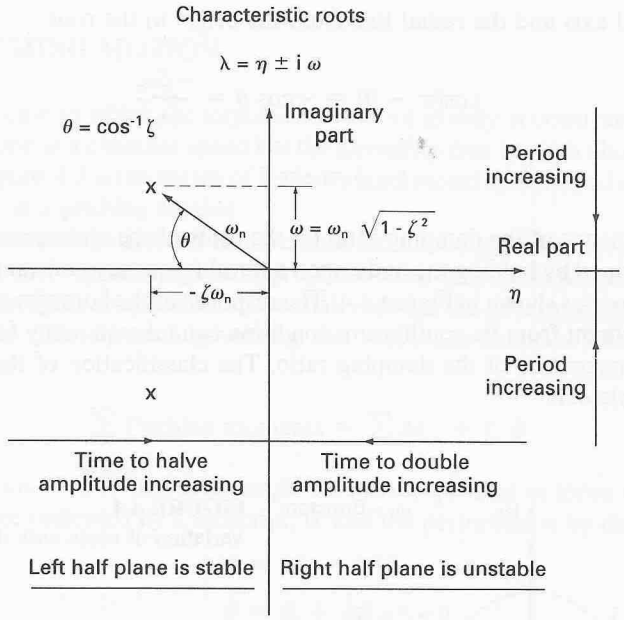

FIGURE 4.3
Relationship among η, ω, ζ, and ω_n.

The characteristic equation for the standard form of the second-order differential equation with constant coefficients can be shown to be

$$\lambda^2 + 2\zeta\omega_n\lambda + \omega_n^2 = 0 \tag{4.21}$$

The roots of the characteristic equation are

$$\lambda_{1,2} = -\zeta\omega_n \pm i\omega_n\sqrt{1 - \zeta^2} \tag{4.22}$$

or

$$\lambda_{1,2} = \eta \pm i\omega \tag{4.23}$$

where

$$\eta = -\zeta\omega_n \tag{4.24}$$

$$\omega = \omega_n\sqrt{1 - \zeta^2} \tag{4.25}$$

The real part of λ, that is, η, governs the damping of the response and the imaginary part, ω, is the damped natural frequency.

Figure 4.3 shows the relationship between the roots of the characteristic equation and η, ω, ζ, and ω_n. When the roots are complex the radial distance from the origin to the root is the undamped natural frequency. The system damping η is the real part of the complex root and the damped natural frequency is the imaginary part of the root. The damping ratio ζ is equal to the cosine of the angle between the

negative real axis and the radial line from the origin to the root:

$$\cos(\pi - \theta) = -\cos\theta = \frac{-\zeta\omega_n}{\omega_n} \tag{4.26}$$

or

$$\zeta = \cos\theta \tag{4.27}$$

The influence of the damping ratio on the roots of the characteristic equation can be examined by holding the undamped natural frequency constant and varying ζ from $-\infty$ to ∞ as shown in Figure 4.4. The response of the homogeneous equation to a displacement from its equilibrium condition can take on many forms depending on the magnitude of the damping ratio. The classification of the response is given in Table 4.1.

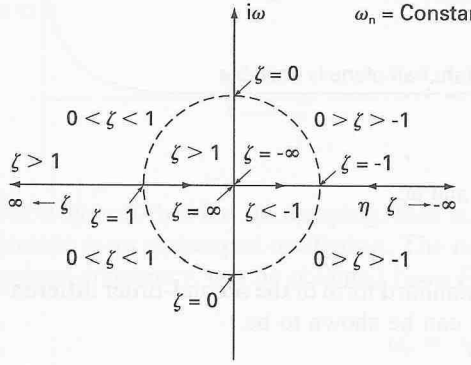

FIGURE 4.4
Variation of roots with damping ratio.

TABLE 4.1
Variation of response with damping ratio

Magnitude of damping ratio	Type of root	Time response
$\zeta < -1$	Two positive real distinct roots	Exponentially growing motion
$0 > \zeta > -1$	Complex roots with a positive real part	Exponentially growing sinusoidal motion
$\zeta = 0$	Complex roots with a real part 0	Undamped sinusoidal motion Pure harmonic motion
$0 < \zeta < 1$	Complex roots with a real part negative	Underdamped exponentially decaying sinusoidal motion
$\zeta = 1$	Two negative equal real roots	Critically damped exponentially decaying motion
$\zeta > 1$	Two negative distinct real roots	Overdamped exponentially decaying motion

4.3 PURE PITCHING MOTION

Consider the case in which the airplane's center of gravity is constrained to move in a straight line at a constant speed but the aircraft is free to pitch about its center of gravity. Figure 4.5 is the sketch of a wind-tunnel model constrained so that it can perform only in a pitching motion.

The equation of motion can be developed from the rigid body equations developed in Chapter 3 by making the appropriate assumptions. However, to aid our understanding of this simple motion, we shall rederive the governing equation from first principles. The equation governing this motion is obtained from Newton's second law:

$$\sum \text{Pitching moments} = \sum M_{cg} = I_y\,\ddot{\theta} \tag{4.28}$$

The pitching moment M and pitch angle θ can be expressed in terms of an initial reference value indicated by a subscript, 0, and the perturbation by the Δ symbol:

$$M = M_0 + \Delta M \tag{4.29}$$

$$\theta = \theta_0 + \Delta\theta \tag{4.30}$$

If the reference moment M_0 is 0, then equation (4.28) reduces to

$$\Delta M = I_y\,\Delta\ddot{\theta} \tag{4.31}$$

For the restricted motion that we are examining, the variables are the angle of attack, pitch angle, the time rate of change of these variables, and the elevator angle. The pitching moment is not a function of the pitch angle but of the other variables and can be expressed in functional form as follows:

$$\Delta M = \text{fn}(\Delta\alpha, \Delta\dot{\alpha}, \Delta q, \Delta\delta_e) \tag{4.32}$$

Equation (4.32) can be expanded in terms of the perturbation variables by means

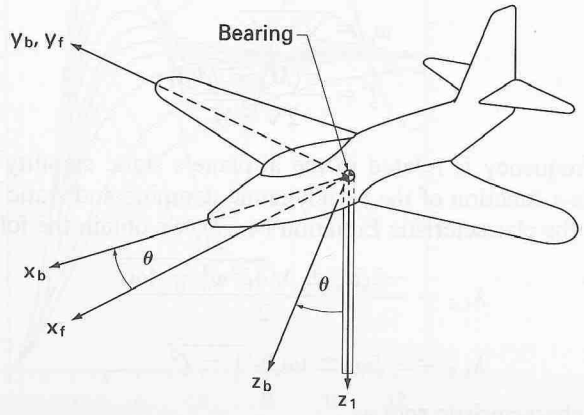

FIGURE 4.5
A model constrained to a pure pitching motion.

of a Taylor series:

$$\Delta M = \frac{\partial M}{\partial \alpha}\Delta\alpha + \frac{\partial M}{\partial \dot{\alpha}}\Delta\dot{\alpha} + \frac{\partial M}{\partial q}\Delta q + \frac{\partial M}{\partial \delta_e}\Delta\delta_e \tag{4.33}$$

If we align the body and fixed frames so they coincide at $t = 0$, the change in angle of attack and pitch angles are identical; that is,

$$\Delta\alpha = \Delta\theta \quad \text{and} \quad \Delta\dot{\theta} = \Delta q = \Delta\dot{\alpha} \tag{4.34}$$

This is true only for the special cases where the center of gravity is constrained. Substituting this information into Equation (4.31) yields

$$\Delta\ddot{\alpha} - (M_q + M_{\dot{\alpha}})\Delta\dot{\alpha} - M_\alpha\Delta\alpha = M_{\delta e}\Delta\delta_e \tag{4.35}$$

where

$$M_q = \frac{\partial M}{\partial q}\Big/ I_y, \qquad M_{\dot{\alpha}} = \frac{\partial M}{\partial \dot{\alpha}}\Big/ I_y, \qquad \text{and so forth}$$

Equation (4.35) is a nonhomogeneous second-order differential equation, having constant coefficients. This equation is similar to a torsional spring-mass-damper system with a forcing function, which was mentioned briefly in the previous section. The static stability of the airplane can be thought of as the equivalent of an aerodynamic spring, while the aerodynamic damping terms are similar to a torsional damping device. The characteristic equation for Equation (4.35) is

$$\lambda^2 - (M_q + M_{\dot{\alpha}})\lambda - M_\alpha = 0 \tag{4.36}$$

This equation can be compared with the standard equation of a second-order system:

$$\lambda^2 + 2\zeta\omega_n\lambda + \omega_n^2 = 0 \tag{4.37}$$

where ζ is the damping ratio and ω_n is the undamped natural frequency. By inspection we see that

$$\omega_n = \sqrt{-M_\alpha} \tag{4.38}$$

and

$$\zeta = \frac{-(M_q + M_{\dot{\alpha}})}{2\sqrt{-M_\alpha}} \tag{4.39}$$

Note that the frequency is related to the airplane's static stability and that the damping ratio is a function of the aerodynamic damping and static stability.

If we solve the characteristic Equation (4.37), we obtain the following roots:

$$\lambda_{1,2} = \frac{-2\zeta\omega_n \pm \sqrt{4\zeta^2\omega_n^2 - 4\omega_n^2}}{2} \tag{4.40}$$

or

$$\lambda_{1,2} = -\zeta\omega_n \pm i\omega_n\sqrt{1-\zeta^2} \tag{4.41}$$

Expressing the characteristic root as

$$\lambda_{1,2} = \eta \pm i\omega \tag{4.42}$$

and comparing Equation (4.42) with (4.41), yields

$$\eta = -\zeta\omega_n \tag{4.43}$$

and

$$\omega = \omega_n\sqrt{1-\zeta^2} \tag{4.44}$$

which are the real and imaginary parts of the characteristic roots. The angular frequency ω is called the damped natural frequency of the system.

The general solution to Equation (4.35) for a step change $\Delta\delta_e$ in the elevator angle can be expressed as

$$\Delta\alpha(t) = \Delta\alpha_{\text{trim}}\left[\left(1 + \frac{e^{-\zeta\omega_n t}}{\sqrt{1-\zeta^2}}\sin(\sqrt{1-\zeta^2}\,\omega_n t + \phi)\right)\right] \tag{4.45}$$

where $\Delta\alpha_{\text{trim}}$ = change in trim angle of attack $= -(M_{\delta_e}\Delta\delta_e)/M_\alpha$

ζ = damping ratio $= -(M_q + M_{\dot{\alpha}})/(2\sqrt{-M_\alpha})$

ω_n = undamped natural frequency $= \sqrt{-M_\alpha}$

ϕ = phase angle $= \tan^{-1}(-\sqrt{1-\zeta^2}/-\zeta)$

The solution is a damped sinusoidal motion with the frequency a function of C_{m_α} and the damping rate a function of $C_{m_q} + C_{m_{\dot{\alpha}}}$ and $C_{m_{\dot{\alpha}}}$. Figure 4.6 illustrates the angle of attack time history for various values of the damping ratio ζ. Note that as the system damping is increased the maximum overshoot of the response diminishes.

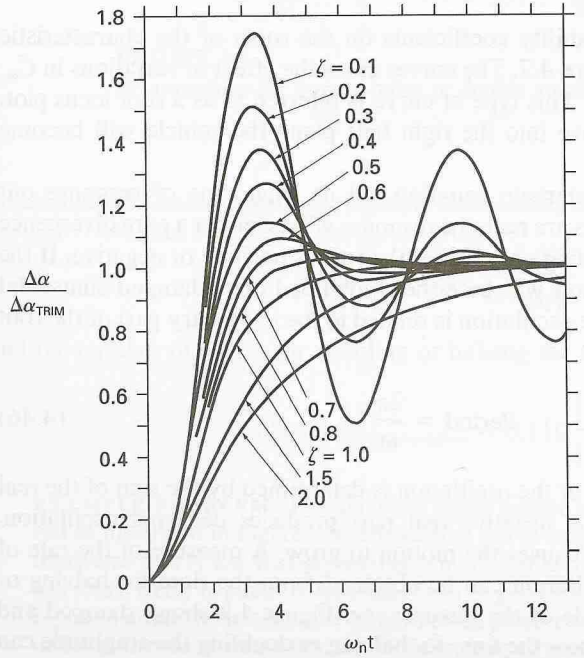

FIGURE 4.6
Angle of attack time history of a pitching model for various damping ratios.

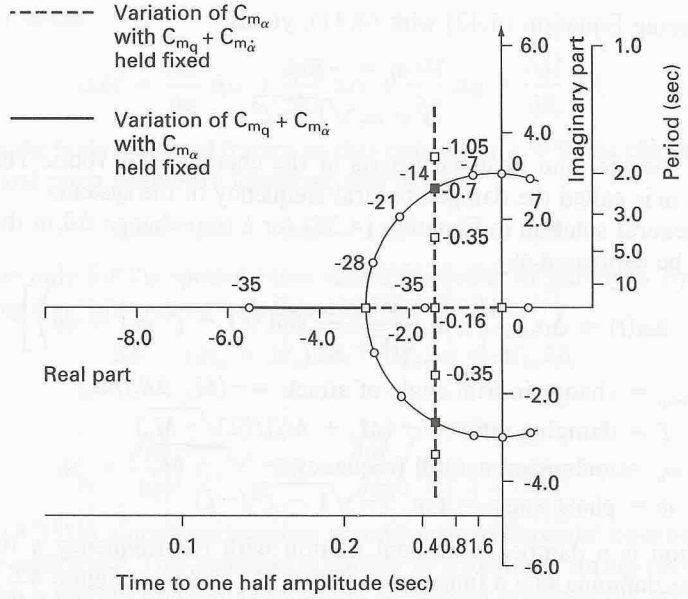

FIGURE 4.7
Variation of the characteristic roots of the pitching motion as a function of the stability coefficients.

The influence of the stability coefficients on the roots of the characteristic equation can be seen in Figure 4.7. The curves show the effect of variations in C_{m_α} and $C_{m_q} + C_{m_{\dot\alpha}}$ on the roots. This type of curve is referred to as a root locus plot. Notice that as the roots move into the right half plane the vehicle will become unstable.

The roots of the characteristic equation tell us what type of response our airplane will have. If the roots are real, the response will be either a pure divergence or a pure subsidence, depending on whether the root is positive or negative. If the roots are complex, the motion will be either a damped or undamped sinusoidal oscillation. The period of the oscillation is related to the imaginary part of the root as follows:

$$\text{Period} = \frac{2\pi}{\omega} \tag{4.46}$$

The rate of growth or decay of the oscillation is determined by the sign of the real part of the complex root. A negative real part produces decaying oscillation, whereas a positive real part causes the motion to grow. A measure of the rate of growth or decay of the oscillation can be obtained from the time for halving or doubling the initial amplitude of the disturbance. Figure 4.8 shows damped and undamped oscillations and how the time for halving or doubling the amplitude can

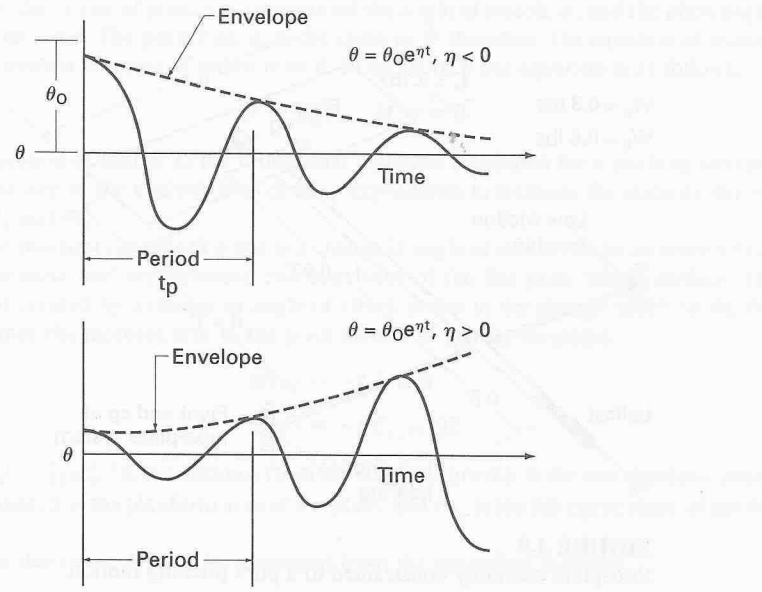

Period	Time to half or double amplitude
$\omega t_p = 2\pi$	$\frac{\theta}{\theta_0} = e^{\eta t}$ or $\ln\frac{\theta}{\theta_0} = \eta t$
$t_p = \frac{2\pi}{\omega}$	$t_{\frac{1}{2}}$ or $t_2 = \frac{0.693}{\lvert\eta\rvert}$

FIGURE 4.8
Relationships for time to halve or double amplitude and the period.

be calculated. The expression for the time for doubling or halving of the amplitude is

$$t_{\text{double}} \quad \text{or} \quad t_{\text{halve}} = \frac{0.693}{|\eta|} \tag{4.47}$$

and the number of cycles for doubling or halving the amplitude is

$$N(\text{cycles})_{\text{double or halve}} = 0.110\,\frac{|\omega|}{|\eta|} \tag{4.48}$$

EXAMPLE PROBLEM 4.1. A flat plate lifting surface is mounted on a hollow slender rod as illustrated in Figure 4.9. The slender rod is supported in the wind tunnel by a transverse rod. A low friction bearing is used so that the slender rod-flat plate system can rotate freely in pitch. To have the center of gravity located at the pivot point ballast is placed inside the slender tube forward of the pivot. Estimate the damping ratio, ζ, the undamped natural frequency, ω_n, and the damped natural frequency of the tube-flat

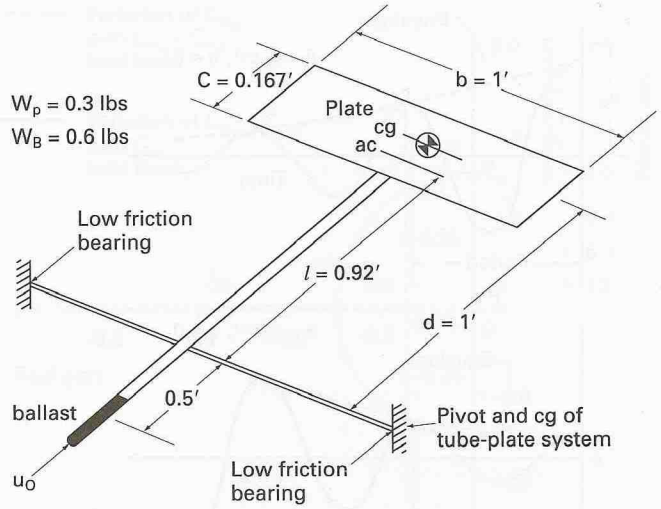

FIGURE 4.9
Rod-plate assembly constrained to a pure pitching motion.

plate assembly. The following assumptions are made in the analysis:

1. Neglect the mass of the slender rod.
2. Neglect the contribution of the pitching moment contribution due to the slender rod.
3. Neglect the mechanical friction of the bearings.

Solution. The equation of motion governing the pitching motion of the slender rod–flat plate model can be derived as follows:

$$\Sigma \text{ Pitching moments about the center of gravity} = I_y\ddot{\theta}$$

$$M = I_y\ddot{\theta}$$

The pitching moment for this model will be a function of only the angle of attack, α, and the pitch rate, q. The contribution due to $\dot{\alpha}$ is not included because this effect is due primarily to the interaction of the wing wake on an aft surface. Because there is no wing in this case the $\dot{\alpha}$ term can be ignored. The aerodynamic pitching moment can be expressed as follows:

$$M = \frac{\partial M}{\partial \alpha}\alpha + \frac{\partial M}{\partial q}q$$

Substituting the moment expression into the differential equation and rearranging yields

$$\ddot{\theta} - M_q q - M_{\dot{\alpha}}\alpha = 0$$

where

$$M_q = \frac{\partial M}{\partial q}\Big/ I_y$$

$$M_\alpha = \frac{\partial M}{\partial \alpha}\Big/ I_y$$

Because the center of gravity is constrained the angle of attack, α, and the pitch angle, θ, are the same. The pitch rate, q, is the same as $\dot{\theta}$; therefore, the equation of motion can be written in terms of either α or θ. In terms of θ the equation is as follows:

$$\ddot{\theta} - M_q\dot{\theta} - M_\alpha\theta = 0$$

This equation is similar to the differential equation developed for a pitching aircraft. The next step in the analysis is to develop expressions to estimate the stability derivatives M_q and M_α.

The moment contribution due to a change in angle of attack can be estimated from the geometric and aerodynamic characteristics of the flat plate lifting surface. The moment created by a change in angle of attack is due to the change in lift on the flat plate times the moment arm to the pivot (center of gravity location).

$$M(\alpha) = -l\,\Delta \text{ Lift}$$

$$M(\alpha) = -l\,C_{L_\alpha}\alpha\,QS$$

where $Q = \frac{1}{2}\rho u_0^2$, l is the distance from the center of gravity to the aerodynamic center of the plate, S is the planform area of the plate, and C_{L_α} is the lift curve slope of the flat plate.

The derivative M_α can be estimated from the preceding formula:

$$M_\alpha = \frac{\partial M}{\partial \alpha}\Big/ I_y = -l\,C_{L_\alpha}QS/I_y$$

In a similar manner the moment contribution due to the pitch rate, q, can be estimated. Recall that when an aft surface undergoes a pitching motion a change in the angle of attack is induced on the surface. The change in angle of attack can be approximated as

$$\tan\alpha = \frac{ql}{u_0}$$

or for small angles

$$\alpha \simeq \frac{ql}{u_0}$$

The pitching moment as a function of q is equal to the change in lift on the aft plate times the moment arm to the center of gravity:

$$M(q) = -l\,C_{L_\alpha}\left(\frac{ql}{u_0}\right)QS$$

The derivative M_q can be estimated from this equation:

$$M_q = \frac{\partial M}{\partial q}\Big/ I_y = -l\,C_{L_\alpha}\left(\frac{l}{u_0}\right)QS/I_y$$

The next step in our analysis it to determine the appropriate values for C_{L_α}, Q, and I_y from the data given. The lift curve slope, C_{L_α}, can be estimated by using the theoretical value of an infinite flat plate, $C_{\ell_\alpha} = 2\pi$/rad and correcting this value for the influence of aspect ratio:

$$C_{L_\alpha} = \frac{C_{\ell_\alpha}}{1 + C_{\ell_\alpha}/(\pi AR)}$$

The flat plate has an aspect ratio of 6, therefore, $C_{L_\alpha} = 4.7/\text{rad}$. The only term in the expression that is not known is the mass moment of inertia, I_y. The inertia of a thin flat plate about the y' axis through the plate's center of gravity is given in terms of ρ, b, t, and c, the mass density of the material and the dimensions of the plate, respectively.

$$I_{y'} = \frac{1}{12}\rho btc^3 = \frac{1}{12}mc^2$$

$$= \frac{1}{12}(9.3 \cdot 10^{-3}\ \text{slugs})(0.167\ \text{ft})^2$$

$$= 2.16 \cdot 10^{-5}\ \text{slug} \cdot \text{ft}^2$$

The inertia of the plate about an axis through the pivot point can be determined using the parallel axis theorem:

$$I_y = I_{y'} + md^2$$

where d is the distance to the new axis:

$$I_y = 2.16 \times 10^{-5}\ \text{slug} \cdot \text{ft}^2 + (9.3 \times 10^{-3}\ \text{slugs})(1\ \text{ft})^2$$

$$= 9.32 \times 10^{-3}\text{slug} \cdot \text{ft}^2$$

The mass moment of inertia of the complete system, flat plate, and ballast is given by

$$I_y = I_{y_{\text{plate}}} + I_{y_{\text{ballast}}}$$

$$= 9.32 \times 10^{-3}\text{slug} \cdot \text{ft}^2 + (1.86 \times 10^{-2}\ \text{slugs})(0.5\ \text{ft})^2$$

$$= 1.4 \times 10^{-2}\text{slug} \cdot \text{ft}^2$$

With the expressions developed for M_α and M_q and the data in Figure 4.9 we now can develop estimates of the derivatives:

$$Q = \frac{1}{2}\rho u_0^2 = (0.5)(0.002378\ \text{slug-ft}^2)(25\ \text{ft/s})^2$$

$$= 0.7\ \text{lb/ft}^2$$

$$M_\alpha = -lC_{L_\alpha}QS/I_y$$

$$= -(0.92\ \text{ft})(4.7/\text{rad})(0.7\ \text{lb/ft}^2)(0.167\ \text{ft}^2)/(1.4 \times 10^{-2}\text{slugs} \cdot \text{ft}^2)$$

$$= -36.1/\text{s}^2$$

and $$M_q = -lC_{L_\alpha}\left(\frac{l}{u_0}\right)QS/I_y$$

$$= -(0.92\ \text{ft})(4.7/\text{rad})[(0.96\ \text{ft})/(25\ \text{ft/s})](0.7\ \text{lb/ft}^2)(0.167\ \text{ft}^2)/$$
$$(1.4 \times 10^{-2}\text{slugs} \cdot \text{ft}^2)$$

$$= -1.38/\text{s}$$

Substituting these values into the differential equation yields

$$\ddot{\theta} + 1.38\,\dot{\theta} + 36.1\theta = 0$$

A second-order differential equation can be expressed in terms of the system damping ratio, ζ, and the system's undamped natural ω_n frequency as follows:

$$\ddot{\theta} + 2\zeta\,\omega_n\dot{\theta} + \omega_n^2\,\theta = 0$$

The system damping ratio and undamped natural frequency can be obtained by inspection:

$$\omega_n^2 = 36.1/\text{s}^2$$

or $$\omega_n = 6.0\ \text{rad/s}$$

and $$2\zeta\omega_n = 1.38$$

$$\zeta = 0.115$$

Finally the damped natural frequency, ω, is obtained from the following equation:

$$\omega = \omega_n\sqrt{1 - \zeta^2}$$

$$= 5.96\ \text{rad/s}$$

In this example problem we have developed the governing differential equation from Newton's second law. The aerodynamic moment was assumed to be linear and a function of α and q and was expressed in terms of stability derivatives. Expressions for estimating the stability derivatives were developed in terms of the aerodynamic, geometric, and inertia characteristics of the rod-plate system.

4.4 STICK FIXED LONGITUDINAL MOTION

The motion of an airplane in free flight can be extremely complicated. The airplane has three translation motions (vertical, horizontal, and transverse), three rotational motions (pitch, yaw, and roll), and numerous elastic degrees of freedom. To analyze the response of an elastic airplane is beyond the scope of this book.

The problem we shall address in this section is the solution of the rigid-body equations of motion. This may seem to be a formidable task; however, some simplifying assumptions will reduce the complexity of the problem. First, we shall assume that the aircraft's motion consists of small deviations from its equilibrium flight condition. Second, we shall assume that the motion of the airplane can be analyzed by separating the equations into two groups. The X-force, Z-force, and pitching moment equations embody the longitudinal equations, and the Y-force, rolling, and yawing moment equations form the lateral equations. To separate the equations in this manner, the longitudinal and lateral equations must not be coupled. These are all reasonable assumptions provided the airplane is not undergoing a large-amplitude or very rapid maneuver.

In aircraft motion studies, one must always be sure that the assumptions made in an analysis are appropriate for the problem at hand. Students are all too eager to use the first equation they can find to solve their homework problems. This type of approach can lead to many incorrect or ridiculous solutions. To avoid such

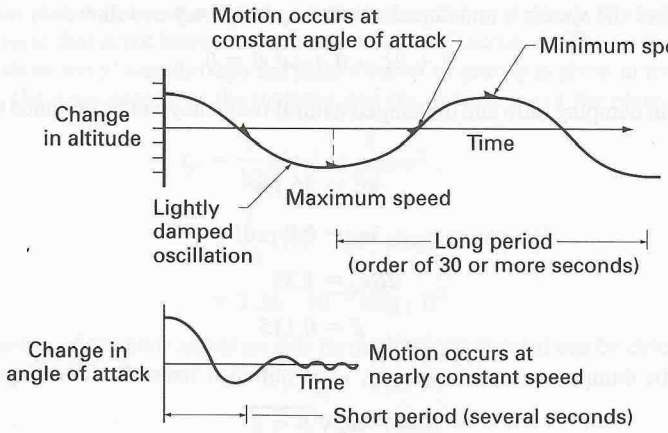

FIGURE 4.10
The phugoid and short-period motions.

embarrassment, one must always verify that the assumptions used in developing the equations one wishes to use are consistent with the problem one is attempting to solve. This is particularly important when solving problems related to aircraft dynamics.

In the following sections we shall examine the longitudinal motion of an airplane without control input. The longitudinal motion of an airplane (controls fixed) disturbed from its equilibrium flight condition is characterized by two oscillatory modes of motion. Figure 4.10 illustrates these basic modes. We see that one mode is lightly damped and has a long period. This motion is called the long-period or phugoid mode. The second basic motion is heavily damped and has a very short period; it is appropriately called the short-period mode.

4.4.1 State Variable Representation of the Equations of Motion

The linearized longitudinal equations developed in Chapter 3 are simple, ordinary linear differential equations with constant coefficients. The coefficients in the differential equations are made up of the aerodynamic stability derivatives, mass, and inertia characteristics of the airplane. These equations can be written as a set of first-order differential equations, called the state-space or state variable equations and represented mathematically as

$$\dot{\mathbf{x}} = \mathbf{A}\mathbf{x} + \mathbf{B}\boldsymbol{\eta} \tag{4.49}$$

where $\mathbf{x}$ is the state vector, $\boldsymbol{\eta}$ is the control vector, and the matrices $\mathbf{A}$ and $\mathbf{B}$ contain the aircraft's dimensional stability derivatives.

The linearized longitudinal set of equations developed earlier are repeated here:

$$\left(\frac{\mathrm{d}}{\mathrm{d}t} - X_u\right)\Delta u - X_w\,\Delta w + (g\cos\theta_0)\,\Delta\theta = X_\delta\,\Delta\delta + X_{\delta_T}\,\Delta\delta_T$$

$$-Z_u\,\Delta u + \left[(1 - Z_{\dot{w}})\frac{\mathrm{d}}{\mathrm{d}t} - Z_w\right]\Delta - \left[(u_0 + Z_q)\frac{\mathrm{d}}{\mathrm{d}t} - g\sin\theta_0\right]\Delta\theta = Z_\delta\,\Delta\delta + Z_{\delta_T}\,\Delta\delta_T \tag{4.50}$$

$$-M_u\,\Delta u - \left(M_{\dot{w}}\frac{\mathrm{d}}{\mathrm{d}t} + M_w\right)\Delta w + \left(\frac{\mathrm{d}^2}{\mathrm{d}t^2} - M_q\frac{\mathrm{d}}{\mathrm{d}t}\right)\Delta\theta = M_\delta\,\Delta\delta + M_{\delta_T}\,\Delta\delta_T$$

where $\Delta\delta$ and $\Delta\delta_T$ are the aerodynamic and propulsive controls, respectively.

In practice, the force derivatives Z_q and $Z_{\dot{w}}$ usually are neglected because they contribute very little to the aircraft response. Therefore, to simplify our presentation of the equations of motion in the state-space form we will neglect both Z_q and $Z_{\dot{w}}$. Rewriting the equations in the state-space form yields

$$\begin{bmatrix}\Delta\dot{u}\\ \Delta\dot{w}\\ \Delta\dot{q}\\ \Delta\dot{\theta}\end{bmatrix} = \begin{bmatrix} X_u & X_w & 0 & -g\\ Z_u & Z_w & u_0 & 0\\ M_u + M_{\dot{w}}Z_u & M_w + M_{\dot{w}}Z_w & M_q + M_{\dot{w}}u_0 & 0\\ 0 & 0 & 1 & 0\end{bmatrix}\begin{bmatrix}\Delta u\\ \Delta w\\ \Delta q\\ \Delta\theta\end{bmatrix} + \begin{bmatrix} X_\delta & X_{\delta_T}\\ Z_\delta & Z_{\delta_T}\\ M_\delta + M_{\dot{w}}Z_\delta & M_{\delta_T} + M_{\dot{w}}Z_{\delta_T}\\ 0 & 0\end{bmatrix}\begin{bmatrix}\Delta\delta\\ \Delta\delta_T\end{bmatrix} \tag{4.51}$$

where the state vector $\mathbf{x}$ and control vector $\boldsymbol{\eta}$ are given by

$$\mathbf{x} = \begin{bmatrix}\Delta u\\ \Delta w\\ \Delta q\\ \Delta\theta\end{bmatrix}, \qquad \boldsymbol{\eta} = \begin{bmatrix}\Delta\delta\\ \Delta\delta_T\end{bmatrix} \tag{4.52}$$

and the matrices $\mathbf{A}$ and $\mathbf{B}$ are given by

$$\mathbf{A} = \begin{bmatrix} X_u & X_w & 0 & -g\\ Z_u & Z_w & u_0 & 0\\ M_u + M_{\dot{w}}Z_u & M_w + M_{\dot{w}}Z_w & M_q + M_{\dot{w}}u_0 & 0\\ 0 & 0 & 1 & 0\end{bmatrix} \tag{4.53}$$

$$\mathbf{B} = \begin{bmatrix} X_\delta & X_{\delta_T}\\ Z_\delta & Z_{\delta_T}\\ M_\delta + M_{\dot{w}}Z_\delta & M_{\delta_T} + M_{\dot{w}}Z_{\delta_T}\\ 0 & 0\end{bmatrix} \tag{4.54}$$

TABLE 4.2
Summary of longitudinal derivatives

$X_u = \dfrac{-(C_{D_u} + 2C_{D_0})QS}{mu_0}$	$X_w = \dfrac{-(C_{D_\alpha} - C_{L_0})QS}{mu_0}$
$Z_u = \dfrac{-(C_{L_u} + 2C_{L_0})QS}{mu_0}$	
$Z_w = \dfrac{-(C_{L_\alpha} + C_{D_0})QS}{mu_0}$	$Z_{\dot{w}} = C_{z_{\dot{\alpha}}} \dfrac{\bar{c}}{2u_0} QS/(u_0 m)$
$Z_\alpha = u_0 Z_w$	$Z_{\dot{\alpha}} = u_0 Z_{\dot{w}}$
$Z_q = C_{Z_q} \dfrac{\bar{c}}{2u_0} QS/m$	$Z_{\delta e} = C_{Z_{\delta e}} QS/m$
$M_u = C_{m_u} \dfrac{(QS\bar{c})}{u_0 I_y}$	
$M_w = C_{m_\alpha} \dfrac{(QS\bar{c})}{u_0 I_y}$	$M_{\dot{w}} = C_{m_{\dot{\alpha}}} \dfrac{\bar{c}}{2u_0} \dfrac{QS\bar{c}}{u_0 I_y}$
$M_\alpha = u_0 M_w$	$M_{\dot{\alpha}} = u_0 M_{\dot{w}}$
$M_q = C_{m_q} \dfrac{\bar{c}}{2u_0} (QS\bar{c})/I_y$	$M_{\delta e} = C_{m_{\delta e}} (QS\bar{c})/I_y$

The force and moment derivatives in the matrices have been divided by the mass of the airplane or the moment of inertia, respectively, as indicated:

$$X_u = \frac{\partial X/\partial u}{m}, \qquad M_u = \frac{\partial X/\partial u}{I_y}, \qquad \text{and so forth} \tag{4.55}$$

Table 4.2 includes a list of the definitions of the longitudinal stability derivatives. Methods for estimating the stability coefficients were discussed in Chapter 3.

The homogeneous solution to Equation (4.49) can be obtained by assuming a solution of the form

$$\mathbf{x} = \mathbf{x}_r e^{\lambda_r t} \tag{4.56}$$

Substituting Equation (4.56) into Equation (4.49) yields

$$[\lambda_r \mathbf{I} - \mathbf{A}]\mathbf{x}_r = 0 \tag{4.57}$$

where $\mathbf{I}$ is the identity matrix

$$\mathbf{I} = \begin{bmatrix} 1 & 0 & 0 & 0 \\ 0 & 1 & 0 & 0 \\ 0 & 0 & 1 & 0 \\ 0 & 0 & 0 & 1 \end{bmatrix} \tag{4.58}$$

For a nontrivial solution to exist, the determinant

$$|\lambda_r \mathbf{I} - \mathbf{A}| = 0 \tag{4.59}$$

must be 0. The roots λ_r of Equation (4.59) are called the characteristic roots or eigenvalues. The solution of Equation (4.59) can be accomplished easily using a digital computer. Most computer facilities will have a subroutine package for determining the eigenvalues of a matrix. The software package MATLAB* was used by the author for solution of matrix problems.

The eigenvectors for the system can be determined once the eigenvalues are known from Equation (4.60).

$$[\lambda_j \mathbf{I} - \mathbf{A}]\mathbf{P}_{ij} = 0 \tag{4.60}$$

where $\mathbf{P}_{ij}$ is the eigenvector corresponding to the jth eigenvalue. The set of equations making up Equation (4.60) is linearly dependent and homogeneous; therefore, the eigenvectors cannot be unique. A technique for finding these eigenvectors will be presented later in this chapter.

EXAMPLE PROBLEM 4.2. Given the differential equations that follow

$$\dot{x}_1 + 0.5x_1 - 10x_2 = -1\delta$$

$$\dot{x}_2 - x_2 + x_1 = 2\delta$$

where x_1 and x_2 are the state variables and δ is the forcing input to the system:

(a) Rewrite these equations in state space form; that is,

$$\dot{\mathbf{x}} = \mathbf{A}\mathbf{x} + \mathbf{B}\boldsymbol{\eta}$$

(b) Find the free response eigenvalues.

(c) What do these eigenvalues tell us about the response of this system?

Solution. Solving the differential equations for the highest order derivative yields

$$\dot{x}_1 = -0.5x_1 + 10x_2 - \delta$$

$$\dot{x}_2 = -x_1 + x_2 + 2\delta$$

or in matrix form

$$\begin{bmatrix} \dot{x}_1 \\ \dot{x}_2 \end{bmatrix} = \begin{bmatrix} -0.5 & 10 \\ -1.0 & 1.0 \end{bmatrix} \begin{bmatrix} x_1 \\ x_2 \end{bmatrix} + \begin{bmatrix} -1 \\ 2 \end{bmatrix} \delta$$

which is the state space formulation

$$\dot{\mathbf{x}} = \mathbf{A}\mathbf{x} + \mathbf{B}\boldsymbol{\eta}$$

where $\mathbf{A} = \begin{bmatrix} -0.5 & 10 \\ -1.0 & 1.0 \end{bmatrix}$ and $\mathbf{B} = \begin{bmatrix} -1 \\ 2 \end{bmatrix}$

The eigenvalues of the system can be determined by solving the equation

$$|\lambda \mathbf{I} - \mathbf{A}| = 0$$

*MATLAB is the trademark for the software package of scientific and engineering computrics produced by The Math Works, Inc.

where **I** is the identity matrix. Substituting the **A** matrix into the preceding equation yields

$$\left|\lambda\begin{bmatrix}1 & 0\\ 0 & 1\end{bmatrix} - \begin{bmatrix}-0.5 & 10\\ -1.0 & 1.0\end{bmatrix}\right| = 0$$

$$\left|\begin{bmatrix}\lambda & 0\\ 0 & \lambda\end{bmatrix} - \begin{bmatrix}-0.5 & 10\\ -1.0 & 1.0\end{bmatrix}\right| = 0$$

$$\begin{vmatrix}\lambda + 0.5 & -10\\ 1.0 & \lambda - 1.0\end{vmatrix} = 0$$

Expanding the determinant yields the characteristic equation

$$(\lambda + 0.5)(\lambda - 1.0) + 10 = 0$$

or

$$\lambda^2 - 0.5\lambda + 9.5 = 0$$

The characteristic equation can be solved for the eigenvalues for the system.

The eigenvalues for this particular characteristic equation are

$$\lambda_{1,2} = 0.25 \pm 3.07\text{i}$$

The eigenvalues are complex and the real part of the root is positive. This means that the system is dynamically unstable. If the system were given an initial disturbance, the motion would grow sinusoidally and the frequency of the oscillation would be governed by the imaginary part of the complex eigenvalue. The time to double amplitude can be calculated from Equation (4.47).

$$t_{\text{double}} = \frac{0.693}{|\eta|} = \frac{0.693}{0.25}$$

$$= 2.77 \text{ s}$$

The period of the sinusoidal motion can be calculated from Equation (4.46).

$$\text{Period} = \frac{2\pi}{\omega} = \frac{2\pi}{3.07} = 2.05 \text{ s}$$

4.5 LONGITUDINAL APPROXIMATIONS

We can think of the long-period or phugoid mode as a gradual interchange of potential and kinetic energy about the equilibrium altitude and airspeed. This is illustrated in Figure 4.10. Here we see that the long-period mode is characterized by changes in pitch attitude, altitude, and velocity at a nearly constant angle of attack. An approximation to the long-period mode can be obtained by neglecting the pitching moment equation and assuming that the change in angle of attack is 0; that is,

$$\Delta\alpha = \frac{\Delta w}{u_0} \qquad \Delta\alpha = 0 \rightarrow \Delta w = 0 \tag{4.61}$$

Making these assumptions, the homogeneous longitudinal state equations reduce to the following:

$$\begin{bmatrix}\Delta\dot{u}\\ \Delta\dot{\theta}\end{bmatrix} = \begin{bmatrix}X_u & -g\\ \dfrac{-Z_u}{u_0} & 0\end{bmatrix}\begin{bmatrix}\Delta u\\ \Delta\theta\end{bmatrix} \tag{4.62}$$

The eigenvalues of the long-period approximation are obtained by solving the equation

$$|\lambda\mathbf{I} - \mathbf{A}| = 0 \tag{4.63}$$

or

$$\begin{vmatrix}\lambda - X_u & g\\ \dfrac{Z_u}{u_0} & \lambda\end{vmatrix} = 0 \tag{4.64}$$

Expanding this determinant yields

$$\lambda^2 - X_u\lambda - \frac{Z_u g}{u_0} = 0 \tag{4.65}$$

or

$$\lambda_p = \left[X_u \pm \sqrt{X_u^2 + 4\frac{Z_u g}{u_0}}\right]\Big/2.0 \tag{4.66}$$

The frequency and damping ratio can be expressed as

$$\omega_{n_p} = \sqrt{\frac{-Z_u g}{u_0}} \tag{4.67}$$

$$\zeta_p = \frac{-X_u}{2\omega_{n_p}} \tag{4.68}$$

If we neglect compressibility effects, the frequency and damping ratios for the long-period motion can be approximated by the following equations:

$$\omega_{n_p} = \sqrt{2}\,\frac{g}{u_0} \tag{4.69}$$

$$\zeta_p = \frac{1}{\sqrt{2}}\frac{1}{L/D} \tag{4.70}$$

Notice that the frequency of oscillation and the damping ratio are inversely proportional to the forward speed and the lift-to-drag ratio, respectively. We see from this approximation that the phugoid damping is degraded as the aerodynamic efficiency (L/D) is increased. When pilots are flying an airplane under visual flight rules the phugoid damping and frequency can vary over a wide range and they will still find the airplane acceptable to fly. On the other hand, if they are flying the airplane under instrument flight rules low phugoid damping will become very objectable. To improve the damping of the phugoid motion, the designer would have to reduce the lift-to-drag ratio of the airplane. Because this would degrade the performance of the airplane, the designer would find such a choice unacceptable and would look for

another alternative, such as an automatic stabilization system to provide the proper damping characteristics.

4.5.1 Short-Period Approximation

An approximation to the short-period mode of motion can be obtained by assuming $\Delta u = 0$ and dropping the X-force equation. The longitudinal state-space equations reduce to the following:

$$\begin{bmatrix} \Delta\dot{w} \\ \Delta\dot{q} \end{bmatrix} = \begin{bmatrix} Z_w & u_0 \\ M_w + M_{\dot{w}}Z_w & M_q + M_{\dot{w}}u_0 \end{bmatrix} \begin{bmatrix} \Delta w \\ \Delta q \end{bmatrix} \tag{4.71}$$

This equation can be written in terms of the angle of attack by using the relationship

$$\Delta\alpha = \frac{\Delta w}{u_0} \tag{4.72}$$

In addition, one can replace the derivatives due to w and $\dot{w}$ with derivatives due to α and $\dot{\alpha}$ by using the following equations. The definition of the derivative M_α is

$$M_\alpha = \frac{1}{I_y}\frac{\partial M}{\partial \alpha} = \frac{1}{I_y}\frac{\partial M}{\partial(\Delta w/u_0)} = \frac{u_0}{I_y}\frac{\partial M}{\partial w} = u_0 M_w \tag{4.73}$$

In a similar way we can show that

$$Z_\alpha = u_0 Z_w \qquad \text{and} \qquad M_{\dot{\alpha}} = u_0 M_{\dot{w}} \tag{4.74}$$

Using these expressions, the state equations for the short-period approximation can be rewritten as

$$\begin{bmatrix} \Delta\dot{\alpha} \\ \Delta\dot{q} \end{bmatrix} = \begin{bmatrix} \dfrac{Z_\alpha}{u_0} & 1 \\ M_\alpha + M_{\dot{\alpha}}\dfrac{Z_\alpha}{u_0} & M_q + M_{\dot{\alpha}} \end{bmatrix} \begin{bmatrix} \Delta\alpha \\ \Delta q \end{bmatrix} \tag{4.75}$$

The eigenvalues of the state equation can again be determined by solving the equation

$$|\lambda \mathbf{I} - \mathbf{A}| = 0 \tag{4.76}$$

which yields

$$\begin{vmatrix} \lambda - \dfrac{Z_\alpha}{u_0} & -1 \\ -M_\alpha - M_{\dot{\alpha}}\dfrac{Z_\alpha}{u_0} & \lambda - (M_q + M_{\dot{\alpha}}) \end{vmatrix} = 0 \tag{4.77}$$

The characteristic equation for this determinant is

$$\lambda^2 - \left(M_q + M_{\dot{\alpha}} + \frac{Z_\alpha}{u_0}\right)\lambda + M_q\frac{Z_\alpha}{u_0} - M_\alpha = 0 \tag{4.78}$$

TABLE 4.3
Summary of longitudinal approximations

	Long period (phugoid)	Short period
Frequency	$\omega_{n_p} = \sqrt{\dfrac{-Z_u g}{u_0}}$	$\omega_{nsp} = \sqrt{\dfrac{Z_\alpha M_q}{u_0} - M_\alpha}$
Damping ratio	$\zeta_p = \dfrac{-X_u}{2\omega_{n_p}}$	$\zeta_{sp} = -\dfrac{M_q + M_{\dot{\alpha}} + \dfrac{Z_\alpha}{u_0}}{2\omega_{n_{sp}}}$

The approximate short-period roots can be obtained easily from the characteristic equation,

$$\lambda_{sp} = \left(M_q + M_{\dot{\alpha}} + \frac{Z_\alpha}{u_0}\right)\Big/2 \pm \left[\left(M_q + M_{\dot{\alpha}} + \frac{Z_\alpha}{u_0}\right)^2 - 4\left(M_q\frac{Z_\alpha}{u_0} - M_\alpha\right)\right]^{1/2}\Big/2 \tag{4.79}$$

or in terms of the damping and frequency

$$\omega_{n_{sp}} = \left[\left(M_q\frac{Z_\alpha}{u_0} - M_\alpha\right)\right]^{1/2} \tag{4.80}$$

$$\zeta_{sp} = -\left[M_q + M_{\dot{\alpha}} + \frac{Z_\alpha}{u_0}\right]\Big/(2\omega_{n_{sp}}) \tag{4.81}$$

Equations (4.80) and (4.81) should look familiar. They are very similar to the equations derived for the case of a constrained pitching motion. If we neglect the Z_α term (i.e., neglect the vertical motion), Equations (4.80) and (4.81) are identical to Equations (4.38) and (4.39). A summary of the approximate formulas is presented in Table 4.3.

To help clarify the preceding analysis, we shall determine the longitudinal characteristics of the general aviation airplane included in Appendix B.

EXAMPLE PROBLEM 4.3. Find the longitudinal eigenvalues and eigenvectors for the general aviation airplane included in Appendix B and Figure 4.11. Compare these results with the answers obtained by using the phugoid and short-period approximations. The exact solution was determined numerically using MATLAB.

Solution. First, we must determine the numerical values of the dimensional longitudinal stability derivatives. The dynamic pressure Q and the terms QS, $QS\bar{c}$, and $\bar{c}/2u_0$ are

$$Q = \tfrac{1}{2}\rho u_0^2 = (0.5)(0.002378 \text{ slug/ft}^3)(176 \text{ ft/s})^2 = 36.8 \text{ lb/ft}^2$$

$$QS = (36.8 \text{ lb/ft}^2)(184 \text{ ft}^2) = 6771 \text{ lb}$$

$$QS\bar{c} = (6771 \text{ lb})(5.7 \text{ ft}) = 38596 \text{ ft} \cdot \text{lb}$$

$$(\bar{c}/2u_0) = (5.7 \text{ ft})/(2 \times 176 \text{ ft/s}) = 0.016 \text{ s}$$

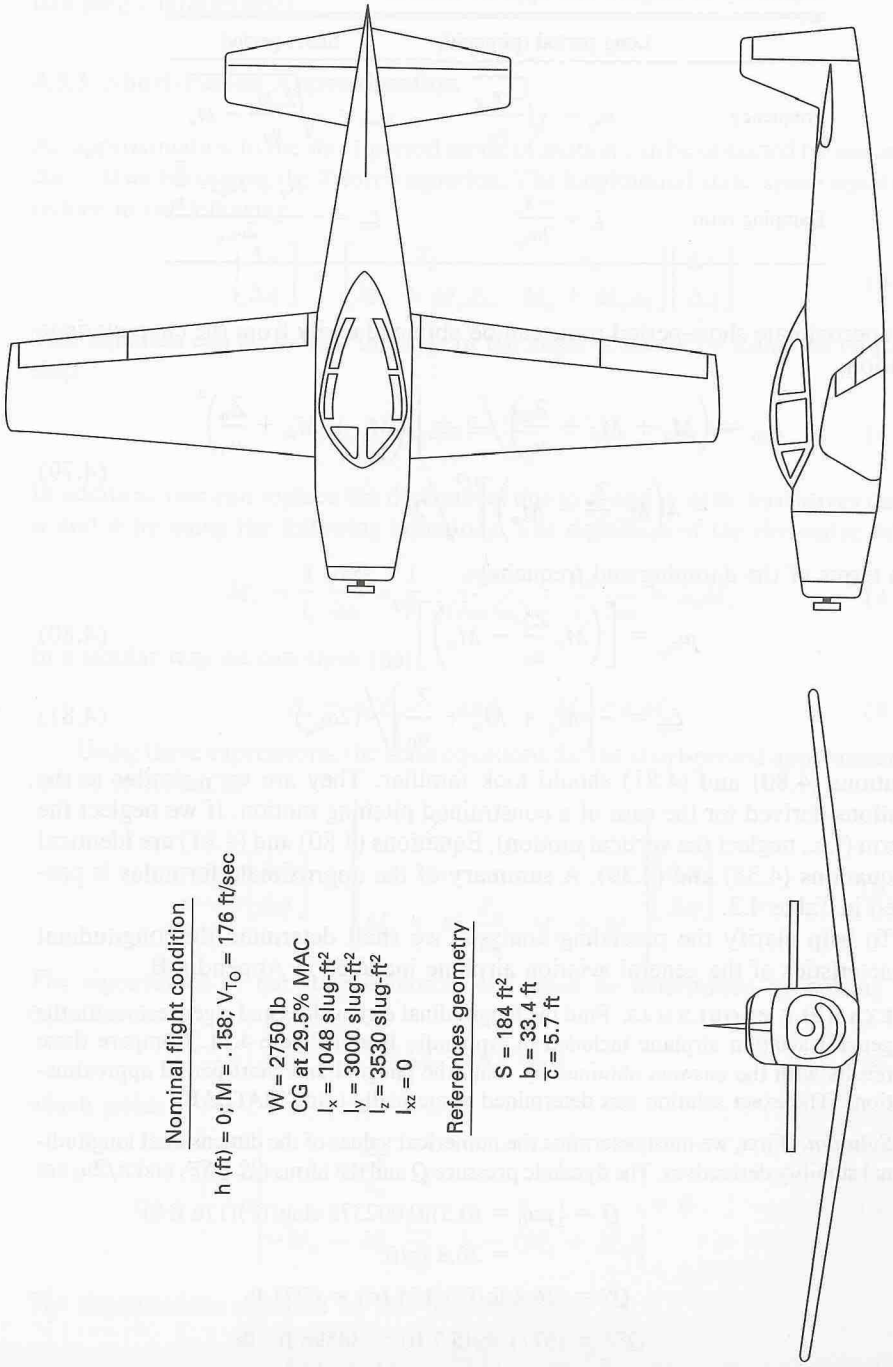

FIGURE 4.11
Geometric, mass, and aerodynamic properties of a general aviation airplane.

The longitudinal derivatives can be estimated from the formulas in Table 4.2.

***u* derivatives**

$$\begin{aligned} X_u &= -(C_{D_u} + 2C_{D_0})QS/(u_0 m) \\ &= -[0.0 + 2(0.05)](6771 \text{ lb})/[(176 \text{ ft/s})(85.4 \text{ slugs})] \\ &= -0.045 \ (\text{s}^{-1}) \\ Z_u &= -(C_{L_u} + 2C_{L_0})QS/(u_0 m) \\ &= -[0.0 + 2(0.41)](6771 \text{ lb})/[(176 \text{ ft/s})(85.4 \text{ slugs})] \\ &= -0.369 \ (\text{s}^{-1}) \\ M_u &= 0 \end{aligned}$$

***w* derivatives**

$$\begin{aligned} X_w &= -(C_{D_\alpha} - C_{L_0})QS/(u_0 m) \\ &= -(0.33 - 0.41)(6771 \text{ lb})/[(176 \text{ ft/s})(85.4 \text{ slugs})] \\ &= 0.036 \ (\text{s}^{-1}) \\ Z_w &= -(C_{L_\alpha} + C_{D_0})QS/(u_0 m) \\ &= -(4.44 + 0.05)(6771 \text{ lb})/[((176 \text{ ft/s})(85.4 \text{ slugs}))] \\ &= -2.02 \ (\text{s}^{-1}) \\ M_w &= C_{m_\alpha} QS\bar{c}/(u_0 I_y) \\ &= (-0.683)(38\,596 \text{ ft} \cdot \text{lb})/[(176 \text{ ft/s})(3000 \text{ slugs} \cdot \text{ft}^2)] \\ &= -0.05 \ [1/(\text{ft} \cdot \text{s})] \end{aligned}$$

***ẇ* derivatives**

$$\begin{aligned} X_{\dot{w}} &= 0 \\ Z_{\dot{w}} &= 0 \\ M_{\dot{w}} &= C_{m_{\dot{\alpha}}} \frac{\bar{c}}{2u_0} QS\bar{c}/(u_0 I_y) \\ &= (-4.36)(0.016 \text{ s})(38\,596 \text{ ft} \cdot \text{lb})/[(176 \text{ ft/s})(3000 \text{ slugs} \cdot \text{ft}^2)] \\ &= -0.0051 \ (\text{ft}^{-1}) \end{aligned}$$

***q* derivatives**

$$\begin{aligned} X_q &= 0 \\ Z_q &= 0 \\ M_q &= C_{m_q} \frac{\bar{c}}{2u_0} QS\bar{c}/I_y \\ &= (-9.96)(0.016 \text{ s})(38\,596 \text{ ft} \cdot \text{lb})/(3000 \text{ slugs} \cdot \text{ft}^2) \\ &= -2.05 \ (\text{s}^{-1}) \end{aligned}$$

Substituting the numerical values of the stability derivatives into Equation (4.51), we can obtain the stability matrix:

$$\dot{\mathbf{x}} = \mathbf{A}\mathbf{x}$$

or

$$\begin{bmatrix} \Delta\dot{u} \\ \Delta\dot{w} \\ \Delta\dot{q} \\ \Delta\dot{\theta} \end{bmatrix} = \begin{bmatrix} -0.045 & 0.036 & 0.0000 & -32.2 \\ -0.369 & -2.02 & 176 & 0.0000 \\ 0.0019 & -0.0396 & -2.948 & 0.000 \\ 0.0000 & 0.0000 & 1.0000 & 0.0000 \end{bmatrix} \begin{bmatrix} \Delta u \\ \Delta w \\ \Delta q \\ \Delta\theta \end{bmatrix}$$

The eigenvalues can be determined by finding eigenvalues of the matrix **A**:

$$|\lambda\mathbf{I} - \mathbf{A}| = 0$$

The resulting characteristic equation is

$$\lambda^4 + 5.05\lambda^3 + 13.2\lambda^2 + 0.67\lambda + 0.59 = 0$$

The solution of the characteristic equation yields the eigenvalues:

$$\lambda_{1,2} = -0.0171 \pm i(0.213) \qquad \text{(phugoid)}$$

$$\lambda_{3,4} = -2.5 \pm i\,(2.59) \qquad \text{(short period)}$$

The period, time, and number of cycles of half amplitude are readily obtained once the eigenvalues are known.

Phugoid (long period)	**Short period**
$t_{1/2} = 0.69/\lvert\eta\rvert = \dfrac{0.69}{-0.0171}$	$t_{1/2} = 0.69/\lvert\eta\rvert = \dfrac{0.69}{-2.5}$
$t_{1/2} = 40.3$ s	$t_{1/2} = 0.28$ s
Period $= 2\pi/\omega = 2\pi/0.213$	Period $= 2\pi/\omega = 2\pi/2.59$
Period $= 29.5$ s	Period $= 2.42$ s
Number of cycles to half amplitude	**Number of cycles to half amplitude**
$N_{1/2} = \dfrac{t_{1/2}}{P} = 0.110\dfrac{\omega}{\lvert\eta\rvert}$	$N_{1/2} = 0.110\dfrac{\omega}{\lvert\eta\rvert}$
$= \dfrac{(0.110)(0.213)}{\lvert-0.0171\rvert}$	$= \dfrac{(0.110)(2.59)}{\lvert-2.5\rvert}$
$N_{1/2} = 1.37$ cycles	$N_{1/2} = 0.11$ cycles

Now let us estimate these parameters by means of the long- and short-period approximations. The damping ratio and undamped natural frequency for the long-period motion was given by Equations (4.69), (4.70), (4.80), and (4.81).

Phugoid approximation

$$\omega_{n_p} = \sqrt{\frac{-Z_u g}{u_0}} = \left[\frac{-(0.369)(32.21)}{(176)}\right]^{1/2} = 0.26 \text{ rad/s}$$

$$\zeta_p = \frac{-X_u}{2\omega_{n_p}} = \frac{-(-0.045)}{2(0.26)} = 0.087$$

$$\lambda_{1,2} = -\zeta_p\omega_{n_p} \pm i\omega_{n_p}\sqrt{1 - \zeta_p^2}$$

$$= -(0.087)(0.26) \pm i(0.26)\sqrt{1 - (0.087)^2}$$

$$= -0.023 \pm i0.26$$

$$\text{Period} = \frac{2\pi}{\omega} = \frac{2\pi}{0.26} = 24.2 \text{ s}$$

$$t_{1/2} = \frac{0.69}{\eta} = \frac{0.69}{|-0.023|} = 30 \text{ s}$$

$$N_{1/2} = 0.110\frac{\omega}{|\eta|} = 0.110\frac{[0.26]}{0.023} = 1.24 \text{ cycles}$$

Short-period approximation

$$\omega_{n_{sp}} = \sqrt{\frac{Z_\alpha M_q}{u_0} - M_\alpha}$$

Recall that $Z_\alpha = u_0 Z_w$, $M_\alpha = u_0 M_w$, and $M_{\dot{\alpha}} = u_0 M_{\dot{w}}$

$$\omega_{n_{sp}} = [(-2.02)(-2.05) - (-0.05)(176)]^{1/2} = 3.6 \text{ rad/s}$$

$$\zeta_{sp} = \left(M_q + M_{\dot{\alpha}} + \frac{Z_\alpha}{u_0}\right) \Big/ [2\omega_{n_{sp}}]$$

$$= [(-2.05) + (-0.88) + (-2.02)]/[(2)(3.6)]$$

$$= 0.69$$

$$\lambda_{1,2,sp} = -\zeta_{sp}\omega_{n_{sp}} \pm i\omega_{n_{sp}}\sqrt{1 - \zeta_{sp}^2}$$

$$= -(0.69)(3.6) \pm i(3.6)\sqrt{1 - (0.69)^2}$$

$$= -2.48 \pm i2.61$$

$$\text{Period} = \frac{2\pi}{\omega} = \frac{2\pi}{2.61} = 2.4 \text{ s}$$

$$t_{1/2} = \frac{0.69}{|\eta|} = \frac{0.69}{|-2.48|} = 0.278 \text{ s}$$

$$N_{1/2} = 0.110\frac{\omega}{|\eta|} = 0.110\frac{3.6}{|-2.48|} = 0.16 \text{ cycles}$$

A summary of the results from the exact and approximate analyses is included in Table 4.4. In this analysis, the short-period approximation was found to be in closer agreement with the exact solution than the phugoid approximation. In general, the short-period approximation is the more accurate one.

The eigenvectors for this problem can be determined by a variety of techniques; however, we will discuss only one relatively straightforward method. For additional

TABLE 4.4
Comparison of exact and aproximate methods

	Exact method	Approximate method	Difference
Phugoid	$t_{1/2} = 40.3$ s	$t_{1/2} = 30$ s	25%
	$P = 29.5$ s	$P = 24.2$ s	18%
Short period	$t_{1/2} = 0.280$ s	$t_{1/2} = 0.278$ s	0%
	$P = 2.42$ s	$P = 2.4$ s	0%

information on other techniques, readers should go to their methematics library or computer center. Most computer facilities maintain digital computer programs suitable for extracting eigenvalues and eigenvectors of large-order systems.

To obtain the longitudinal eigenvectors for this example problem, we will start with Equation (4.60), which is expanded as follows:

$$(\lambda_j - A_{11})\,\Delta u_j - A_{12}\,\Delta w_j - A_{13}\,\Delta q_j - A_{14}\,\Delta\theta_j = 0$$
$$-A_{21}\,\Delta u_j + (\lambda_j - A_{22})\Delta w_j - A_{23} q_j - A_{24}\Delta\theta_j = 0$$
$$-A_{31}\Delta u_j - A_{32}\Delta w_j + (\lambda_j - A_{33})\Delta q_j - A_{34}\Delta\theta_j = 0$$
$$-A_{41}\,\Delta u_j - A_{42}\,\Delta w_j - A_{43}\,\Delta q_j + (\lambda_j - A_{44})\Delta\theta_j = 0$$

In this set of equations, the only unknowns are the components of the eigenvector; the eigenvalues λ_j and the elements of the A matrix were determined previously. Dividing the preceding equations by any one of the unknowns (for this example we will use $\Delta\theta_j$), we obtain four equations for the three unknown ratios. Any three of the four equations can be used to find the eigenvectors. If we drop the fourth equation, we will have a set of three equations with the three unknown ratios, as follows:

$$(\lambda_j - A_{11})\left(\frac{\Delta u}{\Delta\theta}\right)_j - A_{12}\left(\frac{\Delta w}{\Delta\theta}\right)_j - A_{13}\left(\frac{\Delta q}{\Delta\theta}\right)_j = A_{14}$$
$$-A_{21}\left(\frac{\Delta u}{\Delta\theta}\right)_j + (\lambda_j - A_{22})\left(\frac{\Delta w}{\Delta\theta}\right)_j - A_{23}\left(\frac{\Delta q}{\Delta\theta}\right)_j = A_{24}$$
$$-A_{31}\left(\frac{\Delta u}{\Delta\theta}\right)_j - A_{32}\left(\frac{\Delta w}{\Delta\theta}\right)_j + (\lambda_j - A_{33})\left(\frac{\Delta q}{\Delta\theta}\right)_j = A_{34}$$

This set of equations can easily be solved by conventional techniques to yield the eigenvector $[\Delta u/\Delta\theta,\ \Delta w/\Delta\theta,\ \Delta q/\Delta\theta,\ 1]$.

The nondimensional eigenvectors for the example problem have been computed and are listed in Table 4.5. The longitudinal modes now can be examined by means of a vector or Argand diagram. The magnitude of the eigenvectors are arbitrary so only the relative length of the vectors is important.

Figure 4.12 is an Argand diagram illustrating the long-period and short-period modes. In this diagram the lengths of the vectors are decreasing exponentially with time, while the vectors are rotating with the angular rate ω. The motion of the airplane can be imagined as the projection of the eigenvectors along the real axis.

On close examination of Figure 4.12, several observations can be made. For the long-period mode, we see that the changes in angle of attack and pitch rate are

TABLE 4.5
Longitudinal eigenvectors for general aviation

Eigenvector	Long period	Short period
	$\lambda = -0.0171 \pm 0.213$i	$\lambda = -2.5 \pm 2.59$i
$\frac{\Delta u/u_0}{\Delta\theta}$	-0.114 ± 0.837i	0.034 ± 0.025i
$\frac{\Delta w/u_0}{\Delta\theta} = \frac{\Delta\alpha}{\Delta\theta}$	0.008 ± 0.05i	1.0895 ± 0.733i
$\frac{\Delta[qc/(2u_0)]}{\Delta\theta}$	-0.000027 ± 0.00347i	-0.039 ± 0.041i

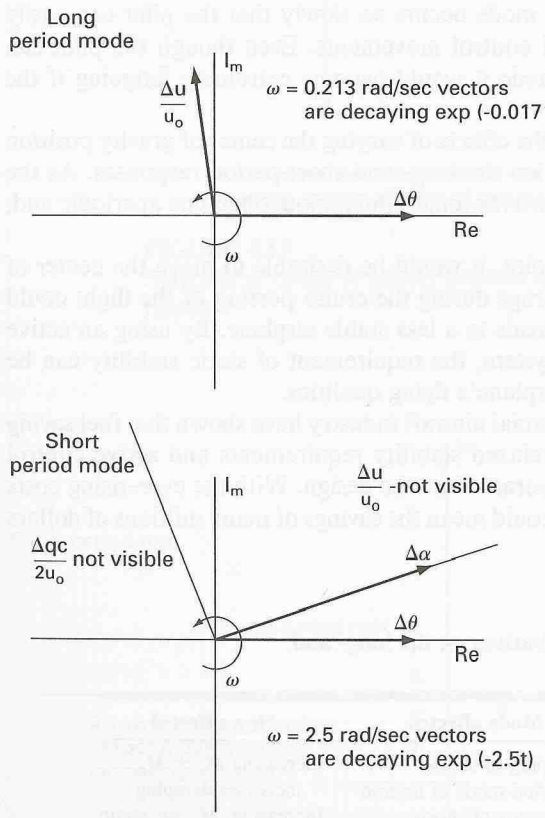

FIGURE 4.12
Eigenvectors for the general aviation airplane in Problem 4.3.

negligible. The motion is characterized by changes in speed and pitch attitude. Notice that the velocity vector leads the pitch attitude by nearly 90° in phase. In contrast, the short-period mode is characterized by changes in angle of attack and pitch attitude with negligible speed variations. As we can see from the vector diagrams, the assumptions we made earlier in developing the long- and short-period approximations indeed are consistent with the exact solution.

4.6 THE INFLUENCE OF STABILITY DERIVATIVES ON THE LONGITUDINAL MODES OF MOTION

The type of response we obtain from solving the differential equations of motion depends on the magnitude of the stability coefficients. This easily can be seen by examining the expressions for the damping ratio and frequency of the long- and short-period approximations. Table 4.6 summarizes the effect of each derivative on the longitudinal motion

Of the two characteristic modes, the short-period mode is the more important. If this mode has a high frequency and is heavily damped, then the airplane will respond rapidly to an elevator input without any undesirable overshoot. When the short-period mode is lightly damped or has a relatively low frequency, the airplane will be difficult to control and in some cases may even be dangerous to fly.

The phugoid or long-period mode occurs so slowly that the pilot can easily negate the disturbance by small control movements. Even though the pilot can correct easily for the phugoid mode it would become extremely fatiguing if the damping were too low.

Figures 4.13 and 4.14 show the effects of varying the center of gravity position and the horizontal tail area size on the long- and short-period responses. As the center of gravity is moved rearward the longitudinal modes become aperiodic and, eventually, unstable.

From a performance standpoint, it would be desirable to move the center of gravity further aft so that trim drags during the cruise portion of the flight could be reduced. Unfortunately, this leads to a less stable airplane. By using an active control stability augmentation system, the requirement of static stability can be relaxed without degrading the airplane's flying qualities.

Recent studies by the commercial aircraft industry have shown that fuel saving of 3 or 4 percent is possible if relaxed stability requirements and active control stability augmentation are incorporated into the design. With the ever-rising costs of jet fuel, this small percentage could mean the savings of many millions of dollars for the commercial airlines.

TABLE 4.6
Influence of stability derivatives on the long- and short-period motions

Stability derivative	Mode affected	How affected
$M_q + M_{\dot{\alpha}}$	Damping of short-period mode of motion	Increasing $M_q + M_{\dot{\alpha}}$ increases damping
M_α	Frequency of short-period mode of motion	Increasing M_α or static stability increases the frequency
X_u	Damping of the phugoid or long-period mode of motion	Increasing X_u increases damping
Z_u	Frequency of phugoid mode of motion	Increasing Z_u increases the frequency

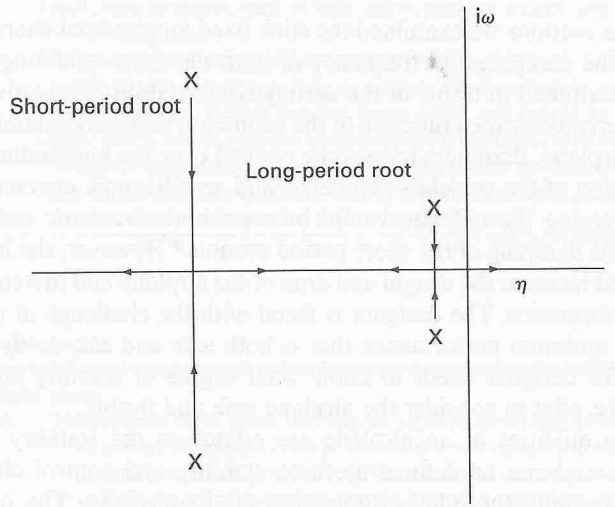

Arrow indicates direction of decreasing static margin. Center of gravity is moving aft.

FIGURE 4.13
Influence of center of gravity position on longitudinal response.

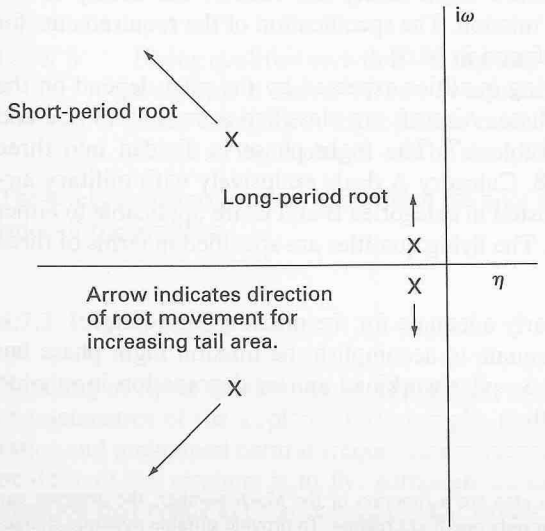

FIGURE 4.14
Influence of horizontal tail area on longitudinal response.

4.7 FLYING QUALITIES

In the previous sections we examined the stick fixed longitudinal characteristics of an airplane. The damping and frequency of both the short- and long-period motions were determined in terms of the aerodynamic stability derivatives. Because the stability derivatives are a function of the geometric and aerodynamic characteristics of the airplane, designers have some control over the longitudinal dynamics by their selection of the vehicle's geometric and aerodynamic characteristics. For example, increasing the tail size would increase both the static stability of the airplane and the damping of the short-period motion.* However, the increased tail area also would increase the weight and drag of the airplane and thereby reduce the airplane's performance, The designer is faced with the challenge of providing an airplane with optimum performance that is both safe and easy to fly. To achieve such a goal, the designer needs to know what degree of stability and control is required for the pilot to consider the airplane safe and flyable.

The flying qualities of an airplane are related to the stability and control characteristics and can be defined as those stability and control characteristics important in forming the pilot's impression of the airplane. The pilot forms a subjective opinion about the ease or difficulty of controlling the airplane in steady and maneuvering flight. In addition to the longitudinal dynamics, the pilot's impression of the airplane is influenced by the feel of the airplane, which is provided by the stick force and stick force gradients. The Department of Defense and Federal Aviation Administration has a list of specifications dealing with airplane flying qualities. These requirements are used by the procuring and regulatory agencies to determine whether an airplane is acceptable for certification. The purpose of these requirements is to ensure that the airplane has flying qualities that place no limitation in the vehicle's flight safety nor restrict the ability of the airplane to perform its intended mission. The specification of the requirements for airplane flying qualities can be found in [4.5].

As one might guess, the flying qualities expected by the pilot depend on the type of aircraft and the flight phase. Aircraft are classified according to size and maneuverability as shown in Table 4.7. The flight phase is divided into three categories as shown in Table 4.8. Category A deals exclusively with military aircraft. Most of the flight phases listed in categories B and C are applicable to either commercial or military aircraft. The flying qualities are specified in terms of three levels:

Level 1 Flying qualities clearly adequate for the mission flight phase.

Level 2 Flying qualities adequate to accomplish the mission flight phase but with some increase in pilot workload and/or degradation in mission effectiveness or both.

* Because the aerodynamic derivatives also are a function of the Mach number, the designer can optimize the dynamic characteristics for only one flight regime. To provide suitable dynamic characteristics over the entire flight envelope, the designer must provide artificial damping by using stability augmentation.

TABLE 4.7
Classification of airplanes

Class I	Small, light airplanes, such as light utility, primary trainer, and light observation craft
Class II	Medium-weight, low-to-medium maneuverability airplanes, such as heavy utility/search and rescue, light or medium transport/cargo/tanker, reconnaissance, tactical bomber, heavy attack and trainer for Class II
Class III	Large, heavy, low-to-medium maneuverability airplanes, such as heavy transport/cargo/tanker, heavy bomber and trainer for Class III
Class IV	High-maneuverability airplanes, such as fighter/interceptor, attack, tactical reconnaissance, observation and trainer for Class IV

TABLE 4.8
Flight phase categories

Nonterminal flight phase	
Category A	Nonterminal flight phase that require rapid maneuvering, precision tracking, or precise flight-path control. Included in the category are air-to-air combat ground attack, weapon delivery/launch, aerial recovery, reconnaissance, in-flight refueling (receiver), terrain-following, antisubmarine search, and close-formation flying
Category B	Nonterminal flight phases that are normally accomplished using gradual maneuvers and without precision tracking, although accurate flight-path control may be required. Included in the category are climb, cruise, loiter, in-flight refueling (tanker), descent, emergency descent, emergency deceleration, and aerial delivery.
Terminal flight phases	
Category C	Terminal flight phases are normally accomplished using gradual maneuvers and usually require accurate flight-path control. Included in this category are takeoff, catapult takeoff, approach, wave-off/go-around and landing.

Level 3 Flying qualities such that the airplane can be controlled safely but pilot workload is excessive and/or mission effectiveness is inadequate or both. Category A flight phases can be terminated safely and Category B and C flight phases can be completed.

The levels are determined on the basis of the pilot's opinion of the flying characteristics of the airplane.

4.7.1 Pilot Opinion

Handling or flying qualities of an airplane are related to the dynamic and control characteristics of the airplane. For example, the short- and long-period damping ratios and undamped natural frequencies influence the pilot's opinion of how easy or difficult the airplane is to fly. Although we can calculate these qualities, the question that needs to be answered is what values should ζ and ω_n take so that the pilot finds the airplane easy to fly. Researchers have studied this problem using ground-based simulators and flight test aircraft. To establish relationships between

TABLE 4.9
Cooper-Harper scale

Pilot rating	Aircraft characteristic	Demand of pilot	Overall assessment
1	Excellent, highly desirable	Pilot compensation not a factor for desired performance	Good flying qualities
2	Good, negligible deficiencies	Pilot compensation not a factor for desired performance	
3	Fair, some mildly unpleasant deficiencies	Minimal pilot compensation required for desired performance	
4	Minor but annoying deficiencies	Desired performance requires moderate pilot compensation	Flying qualities warrant improvement
5	Moderately objectionable deficiencies	Adequate performance requires considerable pilot compensation	
6	Very objectionable but tolerable deficiencies	Adequate performance requires extensive pilot compensation	
7	Major deficiencies	Adequate performance not attainable with maximum tolerable pilot compensation; controllability not in question	Flying quality deficiencies require improvement
8	Major deficiencies	Considerable pilot compensation is required for control	
9	Major deficiencies	Intense pilot compensation is required to retain control	
10	Major deficiencies	Control will be lost during some portion of required operation	Improvement mandatory

the stability and control parameters of the airplane and the pilot's opinion of the airplane a pilot rating system was developed. A variety of rating scales have been used over the years; however, the rating system proposed by Cooper and Harper [4.6] has found widespread acceptance. The Cooper-Harper scale is presented in Table 4.9. The rating scale goes from 1 to 10 with low numbers corresponding to good flying or handling qualities. The scale is an indication of the difficulty in achieving the desired performance that the pilot expects.

Flying qualities research provides the designer information to assess the flying qualities of a new design early in the design process. If the flying qualities are found to be inadequate then the designer can improve the handing qualities by making design changes that influence the dynamic characteristics of the airplane. A designer that follows the flying qualities guidelines can be confident that when the airplane finally is built it will have flying qualities acceptable to its pilots.

Extensive research programs have been conducted by the government and the aviation industry to quantify the stability and control characteristics of the airplane with the pilot's opinion of the airplane's flying qualities. Figure 4.15 is an example of the type of data generated from flying qualities research. The figure shows the relationship between the level of flying qualities and the damping ratio and undamped natural frequency of the short-period mode. This kind of figure is sometimes referred to as a thumbprint plot. Table 4.10 is a summary of the longitudinal

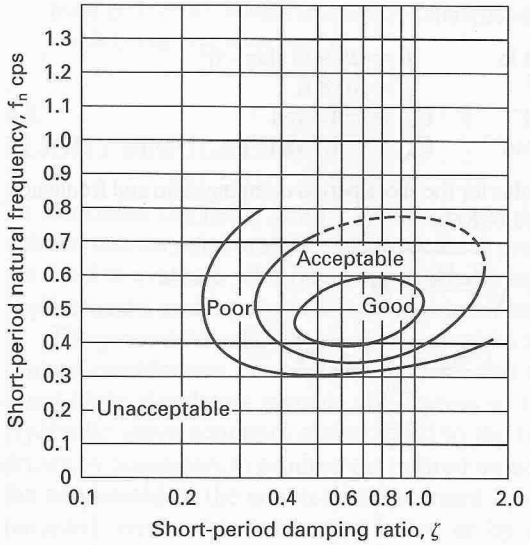

FIGURE 4.15
Short-period flying qualities.

TABLE 4.10
Longitudinal flying qualities

Phugoid mode		
Level 1	$\zeta > 0.04$	
Level 2	$\zeta > 0$	
Level 3	$T_2 > 55$ s	

Short-period mode				
	Categories A and C		**Category B**	
Level	ζ_{sp} min	ζ_{sp} max	ζ_{sp} min	ζ_{sp} max
1	0.35	1.30	0.3	2.0
2	0.25	2.00	0.2	2.0
3	0.15	—	0.15	—

specifications for the phugoid and short-period motions that is valid for all classes of aircraft.

The information provided by Table 4.10 provides the designer with valuable design data. As we showed earlier, the longitudinal response characteristics of an airplane are related to its stability derivatives. Because the stability derivatives are related to the airplane's geometric and aerodynamic characteristics it is possible for the designer to consider flying qualities in the preliminary design phase.

EXAMPLE PROBLEM 4.4. A fighter aircraft has the aerodynamic, mass, and geometric characteristics that follow. Determine the short-period flying qualities at sea level, at 25,000 ft, and at 50,000 ft for a true airspeed of 800 ft/s. How can the designer

improve the flying qualities of this airplane?

$$W = 17\,580 \text{ lb} \qquad I_y = 25\,900 \text{ slug} \cdot \text{ft}^2$$
$$S = 260 \text{ ft}^2 \qquad \bar{c} = 10.8 \text{ ft}$$
$$C_{L_\alpha} = 4.0 \text{ rad}^{-1} \qquad C_{m_q} = -4.3 \text{ rad}^{-1}$$
$$C_{m_\alpha} = -0.4 \text{ rad}^{-1} \qquad C_{m_{\dot{\alpha}}} = -1.7 \text{ rad}^{-1}$$

Solution. The approximate formulas for the short-period damping ratio and frequency are given by Equations (4.80) and (4.81):

$$\omega_{n_{sp}} = \sqrt{\frac{Z_\alpha M_q}{u_0} - M_\alpha}$$

$$\zeta_{sp} = -\frac{(M_q + M_{\dot{\alpha}} + Z_\alpha/u_0)}{2\omega_{n_{sp}}}$$

where $Z_\alpha = -C_{L_\alpha} QS/m$

$$M_q = C_{m_q}\left(\frac{\bar{c}}{2u_0}\right)\frac{QS\bar{c}}{I_y}$$

$$M_\alpha = C_{m_\alpha}\frac{QS\bar{c}}{I_y}$$

$$M_{\dot{\alpha}} = C_{m_{\dot{\alpha}}}\left(\frac{\bar{c}}{2u_0}\right)\frac{QS\bar{c}}{I_y}$$

If we neglect the effect of Mach number changes in the stability coefficients, the damping ratio and frequency can easily be calculated from the preceding equations. Figure 4.16 is a plot of ζ_{sp} and $\omega_{n_{sp}}$ as functions of the altitude. Comparing the estimated short-period damping ratio and frequency with the pilot opinion contours in Figure 4.15, we see that this airplane has poor handling qualities at sea level that deteriorate to unacceptable characteristics at altitude.

To improve the flying qualities of this airplane, the designer needs to provide more short-period damping. This could be accomplished by increasing the tail area or the tail moment arm. Such geometric changes would increase the stability coefficients C_{m_α}, C_{m_q}, and $C_{m_{\dot{\alpha}}}$. Unfortunately, this cannot be accomplished without a penalty in flight performance. The larger tail area results in increased structural weight and empennage drag. For low-speed aircraft geometric design changes usually can be used to provide suitable flying qualities; for aircraft that have an extensive flight envelope such as fighters it is not possible to provide good flying qualities over the entire flight regime

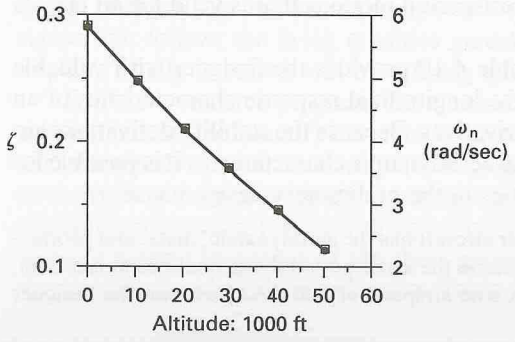

FIGURE 4.16
Variation of ζ_{sp} and $\omega_{n_{sp}}$ as a function of altitude.

from geometric considerations alone. This can be accomplished, however, by using a stability augmentation system.

4.8 FLIGHT SIMULATION

To determine the flying quality specifications described in a previous section requires some very elaborate test facilities. Both ground-based and in-flight simulators are used to evaluate pilot opinion on aircraft response characteristics, stick force requirements, and human factor data such as instrument design, size, and location.

The ground-based flight simulator provides the pilot with the "feel" of flight by using a combination of simulator motions and visual images. The more sophisticated flight simulators provide six degrees of freedom to the simulator cockpit. Hydraulic servo actuators are attached to the bottom of the simulator cabin and driven by computers to produce the desired motion. The visual images produced on the windshield of the simulator are created by projecting images from a camera mounted over a detailed terrain board or by computer-generated images. Figure 4.17 is a sketch of a five degree of freedom ground-based simulator used by the

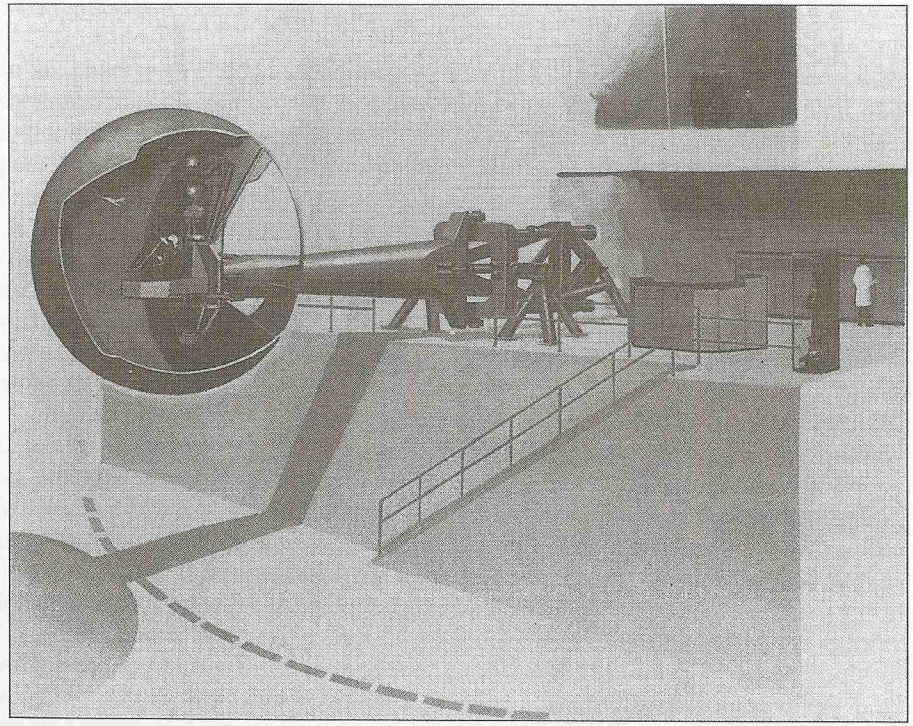

FIGURE 4.17
Sketch of United States Air Force Large Amplitude Multimode Aerospace Research Simulator (LAMARS). Courtesy of the Flight Control Division, Flight Dynamics Directorate, Wright Laboratory.

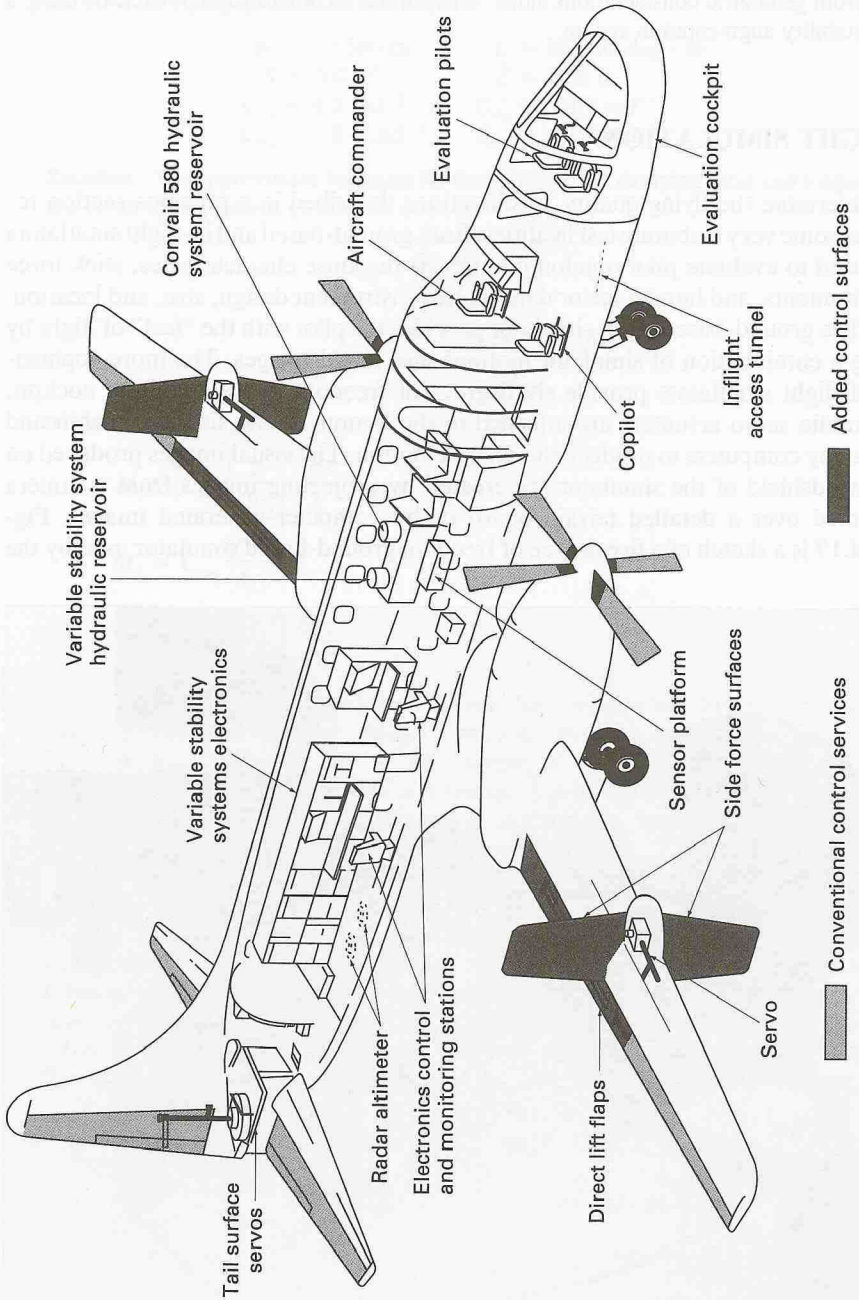

FIGURE 4.18
Airborne flight simulator.

United States Air Force for handling qualities research. The crew station is located at the end of a 30 ft arm that can be controlled to provide the crew with vertical and lateral accelerations.

An example of an in-flight simulator is shown in Figure 4.18. This figure is a sketch of the U.S. Air Force's total in-flight simulator (TIFS), which is a modified C131 transport. By using special force-producing control surfaces such as direct lift flaps and side force generators, this airplane can be used to simulate a wide range of larger aircraft. The TIFS has been used to simulate the B-1, C-5, and space shuttle among other craft.

The stability characteristics of the simulator can be changed through the computer. This capability permits researchers to establish the relationship between pilot opinion and aircraft stability characteristics. For example, the short-period characteristics of the simulator could be varied and the simulator pilot would be asked to evaluate the ease or difficulty of flying the simulator. In this manner, the researcher can establish the pilot's preference for particular airplane response characteristics.

4.9 SUMMARY

In this chapter we examined the stick fixed longitudinal motion of an airplane using the linearized equations of motion developed in Chapter 3. The longitudinal dynamic motion was shown to consist of two distinct and separate modes: a long-period oscillation that is lightly damped, and a very short-period but heavily damped oscillation.

Approximate relationships for the long- and short-period modes were developed by assuming that the long-period mode occurred at constant angle of attack and the short-period mode occurred at a constant speed. These assumptions were verified by an examination of the exact solution. The approximate formulas permitted us to examine the relationship of the stability derivatives on the longitudinal motion.

Before concluding, it seems appropriate to discuss several areas of research that will affect how we analyze aircraft motions. As mentioned, active control technology in commercial aircraft can be used to improve aerodynamic efficiency. With active controls, the aircraft can be flown safely with more aft center of gravity position than would be possible with a standard control system. By shifting the center of gravity further aft, the trim drag can be reduced substantially. This allows for improved fuel economy during the cruise portion of the flight.

Active control technology also can be used to improve ride comfort and reduce wing bending during flight in turbulent air. With active controls located on the wing, a constant load factor can be maintained. This alleviates most of the unwanted response associated with encounters with a vertical gust field. In addition to improving the ride for passengers, the gust alleviation system reduces the wing bending moments, which means the wing can be lighter. Again, this will result in potential fuel savings.

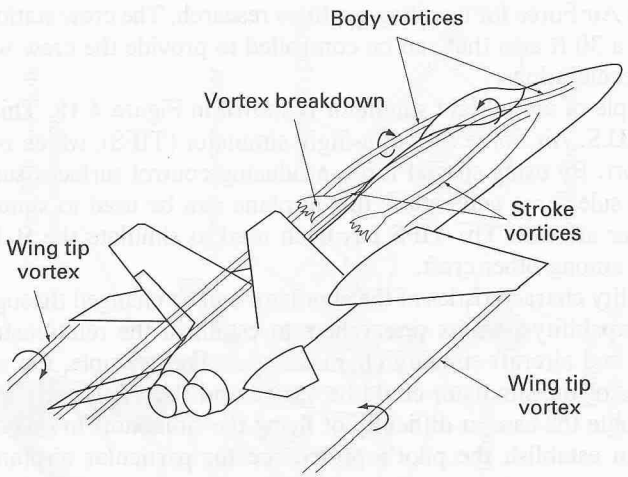

FIGURE 4.19
Sketch of a fighter aircraft illustrating separated vortical flows.

The analysis presented in this chapter assumes that the aerodynamic characteristics are linear and can be represented by stability derivatives. This assumption is quite good if the angle of attack of the airplane is small. However, modern fighter aircraft are capable of performing transient maneuvers that involve high angular rates and large angles of attack [4.7, 4.8]. The flow field around a slender fighter aircraft at large angles of attack is dominated by vortices created by flow separation around the forebody (nose of the fuselage), strake, wing and control surfaces. Figure 4.19 is a sketch of the leeward wake over a slender fighter aircraft. The interaction of these vortices with various components of the aircraft can create significant nonlinear aerodynamic forces and moments. To further illustrate the complexity of the wake flow around a fighter aircraft, we will examine the separated flow over the forebody that is the nose region of the fuselage in the next section.

As the angle of attack of the airplane increases, the flow around the fuselage separates. The separated flow field can cause nonlinear static and dynamic aerodynamic characteristics. An example of the complexity of the leeward wake flows around a slender aircraft and a missile is sketched in Figure 4.20. Notice that as the angle of attack becomes large the separated body vortex flow can become asymmetric. The occurence of this assymetry in the flow can give rise to large side forces, yawing, and rolling moments on the airplane or missile even though the vehicle is performing a symmetric maneuver (i.e., sideslip angle equals 0). The asymmetric shedding of the nose vortices is believed to be a major contribution to the stall spin departure characteristics of many high-performance airplanes.

Figure 4.21 a and b are multiple exposure photographs of the vortex pattern above a cone finned model. A laser light sheet is used to illuminate smoke entrained into the body vortices. The light sheet was positioned so that it intersected the flow normal to the longitudinal axis of the model. The cross section of the body vortices are observed at several axial locations along the model. The model was painted

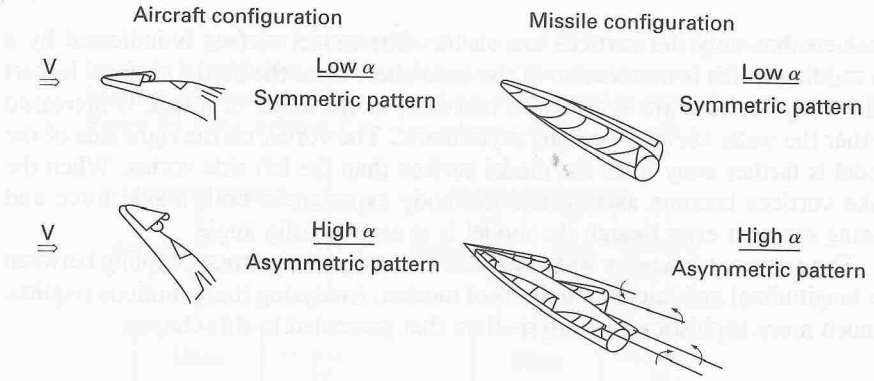

FIGURE 4.20
Vortex flows around an aircraft at large angles of attack.

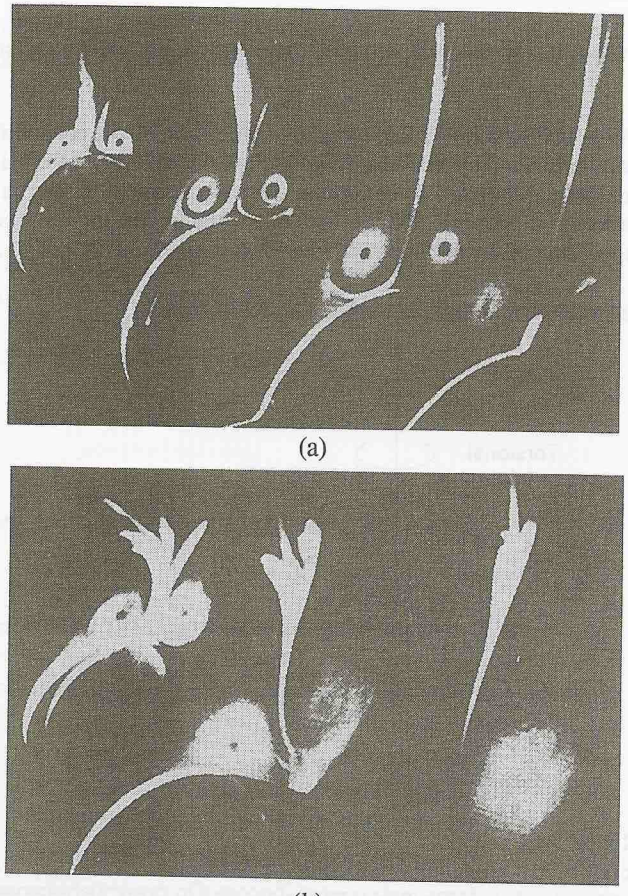

(a)

(b)

FIGURE 4.21
Flow visualization of body vortices. (a) Symmetric body vortex pattern. (b) Asymmetric body vortex pattern.

black so that only the vortices are visible. The model surface is indicated by a curved line which is a reflection of the laser sheet from the model surface. In part a the body vortices are symmetric; however, as the angle of attack is increased further the wake vortices become asymmetric. The vortex on the right side of the model is farther away from the model surface than the left side vortex. When the wake vortices become asymmetric the body experiences both a side force and yawing moment even though the model is at zero sideslip angle.

The asymmetric vortex wake can lead to aerodynamic cross-coupling between the longitudinal and lateral equations of motion. Analyzing these motions requires a much more sophisticated analysis than that presented in this chapter.

PROBLEMS

Problems that require the use of a computer have the capital letter C after the problem number

4.1. Starting with Newton's second law of motion, develop the equation of motion for the simple torsional pendulum shown in Figure P4.1. The concept of the torsional pendulum can be used to determine the mass moment of inertia of aerospace vehicles or components. Discuss how one could use the torsional pendulum concept to determine experimentally the mass moment of inertia of a test vehicle.

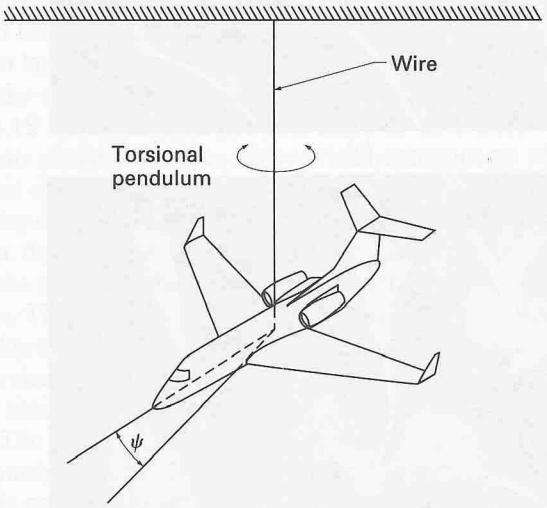

FIGURE P4.1
Aircraft model swinging as a torsional pendulum.

4.2. A mass weighing 5 lb is attached to a spring as shown in Figure P4.2 (a). The spring is observed to extend 1 in. when the mass is attached to the spring. Suppose

the mass is given an instantaneous velocity of 10 ft/s in the downward direction from the equilibrium position. Determine the displacement of the mass as a function of time. Repeat your analysis for the spring mass damper system in Figure P4.2 (b), assume $F = -c\dot{y}$, where $c = 0.6$ (lb · s/ft.).

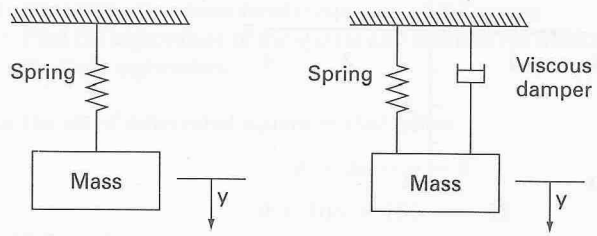

(a) Mass-spring system (b) Mass-spring-damper-system

FIGURE P4.2
Spring-mass and spring-mass-damper systems.

4.3. The differential equation for the constrained center of gravity pitching motion of an airplane is computed to be

$$\ddot{\alpha} + 4\dot{\alpha} + 36\alpha = 0$$

Find the following:
(a) ω_n, natural frequency, rad/s
(b) ζ, damping ratio
(c) ω_d, damped natural frequency, rad/s

4.4. Given the second-order differential equation

$$\ddot{\theta} + 2\dot{\theta} + 5\theta = -\delta$$

(a) Rewrite this equation in the state space form:

$$\dot{\mathbf{x}} = \mathbf{A}\mathbf{x} + \mathbf{B}\boldsymbol{\eta}$$

(c) Determine the eigenvalues of the A matrix.

4.5(C). Determine the eigenvalues and eigenvectors for the following matrix:

$$\mathbf{A} = \begin{bmatrix} 2 & -3 & 1 \\ 3 & 1 & 2 \\ -5 & 2 & -4 \end{bmatrix}$$

4.6. The characteristic roots of a second-order system are shown in Figure P4.6. If this system is disturbed from equilibrium, find the time to half-amplitude, the number of cycles to half amplitude, and the period of motion.

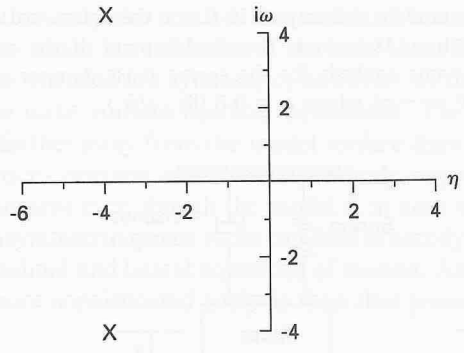

FIGURE P4.6
Second-order system roots.

4.7(C). The missile shown in Figure P4.7 is considered so that only a pitching motion is possible. Assume that the aerodynamic damping and static stability come completely from the tail surface (i.e., neglect the body contribution). If the model is displaced 10° from its trim angle of attack ($\alpha_t = 0$) and then released determine the angle of attack time history. Plot your results. What effect would moving the center of gravity have on the motion of the model?

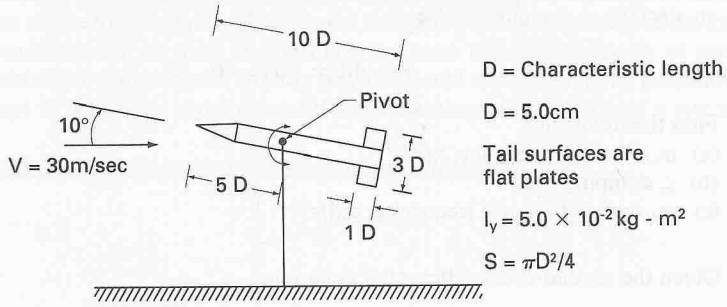

FIGURE P4.7
Pitching wind-tunnel model.

4.8. Develop the equation of motion for an airplane that has freedom only along the flight path; that is, variations in the forward speed. Assume that $X = \text{fn}\ (u, \delta_T)$, where u is the forward speed and δ_T is the propulsive control. If the airplane is perturbed from its equilibrium state, what type of motion would you expect?

4.9. Given the following differential equation

$$\dddot{x} + \ddot{x} - 4\dot{x} + 6x = r$$

(a) Rewrite the equation in state-space form; that is, $\dot{\mathbf{x}} = \mathbf{A}\mathbf{x} + \mathbf{B}\eta$. Hint: let $x_1 = x$, $x_2 = \dot{x}$, $x_3 = \ddot{x}$.

(b) If the characteristic equation is given by

$$(\lambda + 3)(\lambda^2 - 2\lambda + 2) = 0$$

describe the free response modes of motion.

4.10. Given the differential equation

$$\frac{d^2x}{dt^2} + 3\frac{dx}{dt} + 2x = 4$$

(a) Rewrite the equation in state-space form.
(b) Determine the characteristic equation of the system
(c) Find the eigenvalues of the system and describe the motion one might expect for these eigenvalues.

4.11(C). For the set of differential equations that follow

$$\dot{\alpha} + 2\alpha - q = 0$$

$$\ddot{\theta} + 10\alpha + 150 = -5\delta$$

(a) Rewrite the equations in state-space form.
(b) Use MATLAB or similar software to determine the eigenvalues of the **A** matrix.
(c) Determine the response of the system to a unit step input. Assume the initial states all are 0.

4.12. Use the short- and long-period approximations to find the damping ratio for the executive jet airplane described in Appendix B.

4.13. Show that if one neglects compressibility effects the frequency and damping ratio for the phugoid mode can be expressed as

$$\omega_{np} = \sqrt{2}\frac{g}{u_0} \quad \text{and} \quad \zeta_p = \frac{1}{\sqrt{2}}\frac{1}{L/D}$$

4.14. From data in Figure P4.14 estimate the time to half-amplitude and the number of cycles for both the short- and long-period modes.

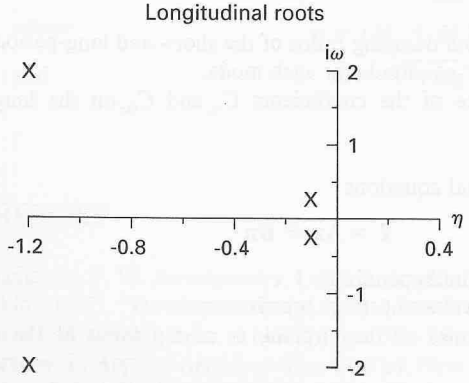

FIGURE P4.14

4.15. The short-period equations for a particular airplane can be expressed as follows:

$$\begin{bmatrix} \Delta\dot{\alpha} \\ \Delta\dot{q} \end{bmatrix} = \begin{bmatrix} \frac{Z_\alpha}{u} & 1 \\ M_\alpha & M_q \end{bmatrix} \begin{bmatrix} \Delta\alpha \\ \Delta q \end{bmatrix}$$

Suppose $Z_\alpha/u_0 = -1$. Determine M_q and M_α so that the damping ration $\zeta = 0$, and the undamped natural frequency is 2 rad/s.

4.16. What effect will increasing altitude have on the short- and long-period modes? Use the approximate formulas in your analysis.

4.17. Develop the equation of motion for an airplane that has freedom only along the flight path; that is, variations in forward speed. If the airplane is perturbed from its equilibrium state what type of motion would you expect? Clearly state all of your assumptions.

4.18(C). Develop a computer program to compute the eigenvalues for the longitudinal equations of motion. Use your program to determine the characteristic roots for the executive jet airplane described in Appendix B. Compare your results with those obtained in Problem 4.12.

4.19(C). An airplane has the following stability and inertia characteristics:

$W = 564\,000$ lb	$C_L = 1.11$
$I_x = 13.7 \times 10^6$ slug · ft^2	$C_D = 0.102$
$I_y = 30.5 \times 10^6$ slug · ft^2	$C_{L_\alpha} = 5.7$ rad^{-1}
$I_z = 43.1 \times 10^6$ slug · ft^2	$C_{D_\alpha} = 0.66$ rad^{-1}
$h =$ sea level	$C_{m_\alpha} = -1.26$ rad^{-1}
$S = 5500$ ft^2	$C_{m_{\dot\alpha}} = -3.2$ rad^{-1}
$b = 195.68$ ft	$C_{m_q} = -20.8$ rad^{-1}
$\bar{c} = 27.3$ ft	
$V = 280$ ft/s	

(a) Find the frequency and damping ratios of the short- and long-period modes.
(b) Find the time to half-amplitude for each mode.
(c) Discuss the influence of the coefficients C_{m_q} and C_{m_α} on the longitudinal motion.

4.20(C). Determine the longitudinal equations

$$\dot{\mathbf{x}} = \mathbf{A}\mathbf{x} + \mathbf{B}\boldsymbol{\eta}$$

for that STOL transport in Appendix B.
(a) Determine the eigenvalues of the **A** matrix.
(b) Determine the response of the airplane to a step input of the elevator, $\Delta\delta_e = -0.1$ rad.

4.21(C). Using the plant matrix **A** determined in Problem 4.18(C), examine the influence of the stability derivatives, C_{m_α}, C_{m_q}, C_{Z_α}, and C_{x_u} on the longitudinal eigenvalues. Vary one stability coefficient at a time and plot the movement of the eigenvalues.

4.22. A wind-tunnel model is constrained so that only a pitching motion can occur. The model is in equilibrium when the angle of attack is 0. When the model is displaced from its equilibrium state and released, the motion shown in Figure P4.22 is

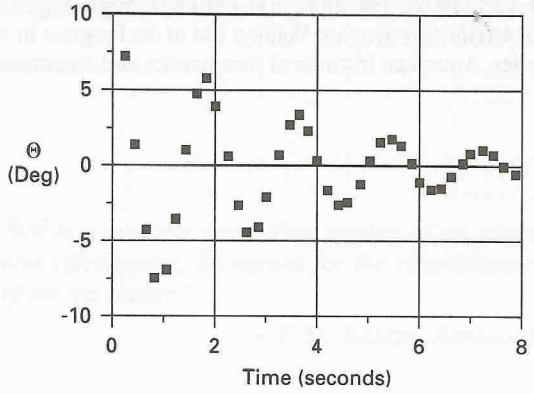

FIGURE P4.22

recorded. Using the following data determine C_{m_α} and $C_{m_q} + C_{m_{\dot\alpha}}$:

$u_0 = 100$ ft/s	$c = 0.2$ ft
$Q = 11.9$ lb/ft^2	$I_y = 0.01$ slug · ft^2
$S = 0.5$ ft^2	

Assume that equation of motion is

$$\theta(t) = \theta_0\, e^{nt} \cos \omega t$$

where $\eta = (M_q + M_{\dot\alpha})/2.0$

and $\omega = \sqrt{-M_\alpha}$

REFERENCES

4.1. Lanchester, F. W. *Aerodonetics*. London: Archibald Constable, 1908.
4.2. Perkins, C. D. "Development of Airplane Stability and Control Technology." *AIAA Journal of Aircraft* 7, no. 4 (1970), pp. 290–301.
4.3. Bairstow, L. *Applied Aerodynamics,* 2nd ed. New York: Longmans, Green, 1939.
4.4. Garber, P. E. "The Wright Brothers' Contribution to Airplane Design" In *Proceedings of the AIAA Diamond Jubilee of Powered Flight—The Evolution of Aircraft Design.* New York: AIAA, 1978.
4.5. *MIL-F-8785B Military Specifications—Flying Qualities of Piloted Airplanes* (August 1969).

4.6. Cooper, G. E. and R. P. Harper. "The Use of Pilot Rating in the Evaluation of Aircraft Handling Qualities." NASA TN D-5153, 1969.
4.7. Kawamura, R. and Aihara, Y. (Editors), *Fluid Dynamics of High Angle of Attack,* Springer-Verlag, New York, NY, 1993.
4.8. Nelson, R. C. "The Role of Flow Visualization in the Study of High-Angle-of-Attack Aerodynamics." *Tactual Missle Aerodyanics,* Volume 104 of the Progress in Astronautics and Aeronautics Series, American Institute of Aeronautics and Astronautics, New York, NY, 1986.